NASA TM X-226



# TECHNICAL MEMORANDUM

## X-226

## A CONCEPT OF A MANNED SATELLITE REENTRY WHICH IS COMPLETED WITH A GLIDE LANDING

By Staff of Langley Flight Research Division
Compiled by Donald C. Cheatham

Langley Research Center
Langley Field, Va.

Declassified May 29, 1961

NATIONAL AERONAUTICS AND SPACE ADMINISTRATION

WASHINGTON

December 1959

NATIONAL AERONAUTICS AND SPACE ADMINISTRATION

TECHNICAL MEMORANDUM X-226

# A CONCEPT OF A MANNED SATELLITE REENTRY WHICH IS COMPLETED WITH A GLIDE LANDING

By Staff of Langley Flight Research Division
Complied by Donald C. Cheatham

## SUMMARY

A concept for a manned satellite reentry from a near space orbit and a glide landing on a normal size airfield is presented. The reentry vehicle configuration suitable for this concept would employ a variable geometry feature in order that the reentry could be made at 90° angle of attack and the landing could be made with a conventional glide approach.

Calculated results for reentry at a flight-path angle of -1° show that with an accuracy of 1 percent in the impulse of a retrorocket, the desired flight-path angle at reentry can be controlled within 0.02° and the distance traveled to the reentry point, within 100 miles. The reentry point is arbitrarily defined as the point at which the satellite passes through an altitude of about 70 miles. Misalinement of the retrorocket by 10° increased these errors by as much as 0.02° and 500 miles. Intra-atmospheric trajectory calculations show that pure drag reentries starting with flight-path angles of -1° or less produce a peak deceleration of 8g. Lift created by varying the angle of attack between 90° and 60° is effective in decreasing the maximum deceleration and allows the range to the "recovery" point (where transition is made from reentry to gliding flight) to be increased by as much as 2,300 miles. A sideslip angle of 30° allows lateral displacement of the flight path by as much as 600 miles.

Reaction controls would provide control-attitude alinement during the orbit phase. For the reentry phase this configuration should have low static longitudinal and roll stability in the 90° angle-of-attack attitude. Control could be effected by leading-edge and trailing-edge flaps.

Transition into the landing phase would be accomplished at an altitude of about 100,000 feet by unfolding the outer wing panels and pitching over to low angles of attack. Calculations indicate that glides can be made from the recovery point to airfields at ranges of from 150 to 200 miles, depending upon the orientation with respect to the original course.

## INTRODUCTION

A study is made of an operational concept whereby a manned satellite reenters the earth's atmosphere from minimum altitude orbits and completes the reentry with a glide approach to a landing. The concept utilizes the advantages of a high drag reentry (see ref. 1) by having the vehicle reenter at angles of attack close to 90°. This high-drag attitude allows much of the kinetic energy to be dissipated in wave drag rather than in surface heating. In addition, tilting the configuration from the 90° angle of attack allows lift or side forces to be developed to control the trajectory. After the high speed, high deceleration and critical-heating phase of the trajectory is passed, the configuration pitches over to low angles of attack and operates as a moderately high lift-drag-ratio glider that would probably have good landing characteristics.

In order to evaluate the feasibility of the operational concept, a study has been made of various aspects of the reentry problem. Because an actual configuration would have design details based upon extensive stability and control studies, only a general description of a possible configuration that could utilize this concept will be given. It is the purpose of this paper to give the results of generalized studies which pertain to the concept.

## SYMBOLS

| | |
|---|---|
| $B$ | constant used in experimental approximation of atmospheric density, $\rho = 0.003e^{-Bh}$ |
| $b$ | wing span, ft |
| $C_L$ | lift coefficient, $\frac{L}{\frac{1}{2}\rho V^2 S}$ |
| $C_R$ | resultant-force coefficient, $\frac{\text{Resultant force}}{\frac{1}{2}\rho V^2 S}$ |
| $D$ | drag force, lb |
| $e$ | Napierian base constant, 2.718 |
| $g$ | acceleration due to gravity at surface of earth, 32.2 ft/sec$^2$ |

| | |
|---|---|
| $h$ | height above surface of earth, ft |
| $I$ | specific impulse, sec |
| $L$ | lift force, lb |
| $M$ | Mach number |
| $m$ | mass, slugs |
| $P$ | atmospheric pressure |
| $p$ | semilatus rectum of an ellipse |
| $q$ | heat-transfer rate, Btu/sec-sq ft |
| $R$ | Universal gas constant |
| $R_e$ | radius of assumed circular earth, ft |
| $R_N$ | radius of hemisphere representing equivalent nose of body, ft |
| $r$ | distance from center of earth, ft |
| $r_1$ | distance from center of earth at retrorocket firing |
| $S$ | surface area, sq ft |
| $ds$ | incremental change in distance, ft |
| $T$ | temperature, $^{o}R$ |
| $t$ | time, sec |
| $V$ | velocity, ft/sec |
| $V_1$ | velocity immediately after firing of retrorocket, ft/sec |
| $V_c$ | velocity in circular orbit |
| $\Delta V$ | velocity decrement, ft/sec |
| $W$ | weight, lb |
| $W_e$ | weight at sea level, lb |

$\alpha$ angle of attack of body X-axis, deg

$\beta$ angle of sideslip, deg

$\delta$ angle between reference axis and resultant velocity vector, deg

$\delta_f$ deflection of control surface, deg

$\epsilon$ elliptic eccentricity

$\gamma$ flight-path angle, deg

$\phi$ inclination of retrorocket thrust axis from horizontal, deg

$\theta$ orbit angle measuring displacements from apogee, deg

$\rho$ atmospheric density, slugs/cu ft

Subscripts:

o initial condition at reentry

1 condition immediately after retrorocket firing

$\infty$ free stream

A dot above a quantity denotes differentiation with respect to time.

## OPERATIONAL CONCEPT

The reentry operation considered in this study is based on the premise that no really fundamental incompatabilities exist between the requirements for an efficient reentry configuration and the requirements for an efficient landing configuration. The reasoning behind this statement becomes apparent as the study progresses.

The space phase of the reentry maneuver is similar to the one usually proposed. The satellite is taken out of orbit by means of a small reduction in tangential velocity (by means of retrothrust) at a predetermined point. Adjustments to the reentry trajectory can be made during the atmospheric part of the reentry. These adjustments can be of the order of thousands of miles along the path and of the order of hundreds of miles lateral to the path.

The problem of severe aerodynamic heating during the deceleration phase of the atmospheric reentry is avoided by achieving very high wave-drag coefficients through extreme bluntness according to principles

discussed in reference 1. The bluntness is obtained by operating a low-aspect-ratio wing near an angle of attack of 90°. The angle of attack can be adjusted through small angles from 90° in order to produce relatively small amounts of lift (with no significant reduction in drag). The lift is used to regulate the accelerations to reasonable values and to adjust the trajectory in order to reach the desired landing point.

At either subsonic or moderate supersonic speeds the angle of attack is reduced to conventional values to provide a glide at a relatively high lift-drag ratio. The transition from reentry to the gliding operation is accomplished by providing a simple variable-geometry feature, which improves the performance in gliding and landing and which assures a stable configuration at gliding speeds. The power-off landing performance of the configuration should be superior to present and proposed research airplanes and most operational jet-fighter airplanes. It is expected that the vehicle could be landed at military airfields and most civil airports.

## CONFIGURATION

The operational concept is based on the premise that the pilot should be able to select his landing area and land without damage to the vehicle. Preferably the vehicle should be capable of landing at any standard airport. In order to obtain reasonable freedom in selecting the landing area during the final gliding phase of the reentry, this phase should be entered at supersonic speed and at a suitably high altitude. This procedure will maximize the energy available for the glide phase. The configuration therefore should have reasonably satisfactory performance and stability and control characteristics as a subsonic or supersonic glider.

For the initial part of the reentry, deceleration should be accomplished with a configuration having an essentially blunt shape exposed to the airstream and a wing loading that is relatively low. Such a configuration would have the maximum ratio of energy dissipation in wave drag to energy dissipation in frictional drag and therefore the least total heat input. Also, such a configuration would permit significant heat dissipation through radiation at allowable structural temperatures. Because the heating of the lower surface under these conditions would be fairly uniform, the design of the heat-absorbing structure would be simplified. With suitable plan-form and housing shape, the configuration under discussion would appear as a blunt body near 90° angle of attack and a relatively efficient glider at low angles of attack.

In order to provide stable characteristics in both regimes of flight, some variable-geometry feature is evidently necessary. For the initial

atmospheric reentry in which the angle of attack is close to 90° the center of gravity must be near the center of area of the configuration in order to avoid large out-of-trim moments. For the gliding configuration, however, the center of gravity must be ahead of the aerodynamic center in order to provide static stability. This change might be accomplished either by reducing an area ahead of the center of gravity or by adding an area behind the center of gravity. In order to improve the subsonic gliding characteristics it appears desirable to utilize added area to increase the span and reduce the wing loading as well as to shift the centroid of area. For this reason the change in geometry which appears most feasible is the unfolding of wing panels located near the rear of the body.

Certain requirements exist for control during each stage of the reentry. First, space controls must be provided to orient the body outside the atmosphere. A retrorocket is required to initiate the reentry and to control the point on the orbit at which the atmosphere is first encountered. During the phase of the reentry in which the angle of attack is close to 90°, aerodynamic damping is negligible and controls in roll, pitch, and yaw are required to provide stability augmentation. Furthermore, control about the three axes would be desirable in order to steer the vehicle and to provide a trajectory with tolerable deceleration. Finally, normal aerodynamic controls would be required for the gliding phase at low angle of attack. Consideration of these requirements indicates the suitability of a modified delta plan-form configuration with wing panels that are folded out only for the gliding phase. Such a configuration could possibly have the general features of the one shown in figure 1(a). Because the details of such a configuration will depend strongly upon extensive stability and control studies, no further description of the configuration will be attempted.

Reentry into the atmosphere is intended to be at an angle of attack near 90° with the outer wing panels folded upward where they will be out of the airstream. The configuration is to be adapted for the gliding phase by unfolding the outer wing panels (fig. 1(b)).

Because of the directional-stability problem and the desire to avoid special structural design on the upper surface of the vehicle to combat aerodynamic heating, it is considered that the maximum Mach number in the gliding condition should be approximately 1.5 to 2. Trajectory calculations show that deceleration to this Mach number or even to low subsonic speeds can readily be accomplished in the 90° angle-of-attack condition. The capability of control at supersonic speeds is desirable, however, in case of some inadvertent separation from the booster during launching and, as mentioned previously, to provide maximum gliding range.

The operational concept of the transition from reentry to the gliding operation does not require that maximum supersonic lift-drag ratios be

obtained. Sufficient attention should be devoted to aerodynamic shape, however, to avoid difficulties due to transonic flow separation or buffeting. The use of a convex lower surface would allow the use of a symmetrical airfoil section which is expected to minimize transonic trim changes.

## TRAJECTORIES

### Transition From Orbit to Atmosphere

The first phase of the reentry from space is the transition from the initial circular orbit to an elliptical orbit which lies at least partly in the upper fringe of the atmosphere. A diagram of this phase is presented in figure 2. The required change in orbit can be accomplished by decreasing the velocity of the vehicle slightly; for example, by firing a retrorocket. Although an initially circular orbit is considered herein, the procedures are qualitatively applicable to elliptical orbits having small eccentricities.

Equations of motion.- The equations of motion which describe the path of the satellite in the reentry phase are

$$V_1 = \sqrt{V_c^2 + \Delta V^2 + 2V_c \Delta V \cos \phi} \tag{1}$$

$$\tan \gamma_1 = \frac{\Delta V \sin \phi}{V_c + \Delta V \cos \phi} \tag{2}$$

$$p = \frac{r_1^2 V_1^2 \cos^2 \gamma_1}{g R_e^2} \tag{3}$$

$$\tan \theta_1 = \tan \gamma_1 \left( \frac{\frac{p}{r_1}}{\frac{p}{r_1} - 1} \right) \tag{4}$$

$$\epsilon = \frac{p - r_1}{r_1 \cos \theta_1} \tag{5}$$

$$\cos \theta = \frac{p - r}{r\epsilon} \tag{6}$$

$$\tan \gamma = \frac{\epsilon \sin \theta}{1 + \epsilon \cos \theta} \tag{7}$$

Effects of retrorocket impulse on transition path.- From the foregoing relations and the assumption of a circular orbit at a height of 150 miles (radius 4,150 miles), computations were made of the effect of rocket impulse on the flight-path angle at a height of 70 miles and on the distance traveled over the earth's surface in descent from orbit to this height. The rocket was assumed to be fired so that the velocity impulse was 180° from the direction of motion. The height of 70 miles was taken as representing the termination of the extra-atmospheric phase of the reentry and the beginning of the atmospheric phase.

The results of the computations are given in figure 3 as plots of reentry angle (flight-path angle at the 70-mile level) and distance traveled over the earth's surface from the point of rocket firing to the reentry at the 70-mile level as a function of the velocity decrement $\Delta V$ produced by the retrorocket. The results indicate that the minimum velocity decrement which will bring the vehicle down to the 70-mile level at perigee is about 125 feet per second. To enter the 70-mile level with a flight-path angle of $-1/2^\circ$ will require a velocity decrement of about 150 feet per second and the reentry will occur at a distance (on the earth's surface) of 9,100 miles beyond the rocket firing point. For a reentry angle of $-1^\circ$, the velocity decrement required will be about 225 feet per second and the distance traveled about 6,600 miles.

The sensitivity of the reentry conditions to the accuracy of the rocket impulse is about 40 miles in distance and $0.01^\circ$ in reentry angle for a 1-percent change in impulse for the $-1^\circ$ reentry angle and about 90 miles and $0.015^\circ$ for the $-1/2^\circ$ reentry angle.

Present solid-fuel rockets can be expected to give total impulses reproducible within about 1 percent at a given temperature. The effect of temperature on the impulse would be about 1 percent for $5^\circ$ temperature variation. It seems reasonable that the rocket temperature could be readily controlled to within $10^\circ$. Variations from the expected impulse might then be 2 to 3 percent. With the range control capabilities of the reentry vehicle, it appears that the effects on the reentry conditions of this uncertainty in the impulse could be compensated for during the atmospheric phase of the reentry.

Effects of variations in reentry height on flight-path angle and distance traveled.- Because of the extremely low densities of the atmosphere in the region of 70 miles altitude, there is some range of choice in assuming the altitude at which the extra-atmospheric phase of the reentry terminates and the atmospheric phase begins. Accordingly, in figure 4, the effects of variations from the nominal height of 70 miles on the entry conditions are given. The reentry flight-path angle at a given height level and the distance to this point from the point of firing the reentry rocket are shown for rocket impulses giving velocity decrements of 225 feet per second and 150 feet per second (corresponding to $-1^\circ$ and $-1/2^\circ$ reentry angles, respectively, at the 70-mile height).

Height variations from the 70-mile level of as much as 5 miles have virtually no effect on the reentry angle for the velocity decrement of 225 feet per second, and would result in a change of only about $0.08^\circ$ for the decrement of 150 feet per second. From results presented subsequently, it will be seen that variations in entry angle of this order have little effect on the computed characteristics of the atmospheric trajectory. A 5-mile variation in height from the 70-mile level would change the distance traveled in the transition from orbit phase by 300 and 500 miles for the decrements of 225 and 150 feet per second, respectively, but this effect would largely be compensated for by corresponding changes in the distance traveled during the intra-atmospheric phase. In other words, variation of the order of 5 miles from the 70-mile height assumed in this study for the junction between the transition from orbit and the intra-atmospheric phase would result in insignificant differences in the overall trajectory characteristics.

Another interpretation of these results is that uncertainty of as much as 5 miles in accounting for diurnal or geographic variations in the effective height of the atmosphere, during the operation of the reentry vehicle, would have little effect on the expected trajectory.

Effects of direction of retrorocket impulse.- As an indication of the degree of accuracy required in alining the retrorocket impulse, the effects of direction of the impulse on distance to entry and angle of entry at the 70-mile level are given in figure 5 for reentry rocket impulses giving vectorial velocity decrements of 225 and 150 feet per second (corresponding to reentry angles of $-1^\circ$ and $-1/2^\circ$ with impulse alined horizontally). It can be seen that the direction of the radial component of the velocity impulse has no effect on the reentry angle because the shape of the final orbit is the same (for a given magnitude of the alinement angle) whether the rocket impulse is toward or away from the earth. However, the apogee of the final orbit is ahead of the rocket firing point if the radial component of the velocity impulse is outward and behind the rocket firing point if the impulse is inward. An outward impulse therefore gives a greater distance to entry than an inward impulse.

It appears from figure 5 that a moderate misalinement of the rocket would have little effect on the reentry angle; a misalinement of as much as $10^\circ$ would reduce the magnitude of the reentry angle by only $0.01^\circ$ to $0.02^\circ$. The effect on the distance from rocket firing point to entry is to increase the distance by 400 and 500 miles for the $-1^\circ$ and $-1/2^\circ$ entry angles, respectively, for a $\phi = 170^\circ$ alinement and to decrease the distance by about 200 to 250 miles for both entry angles for $\phi = 190^\circ$. The glide-control capability of the vehicle in the atmosphere would permit compensation for variations in the entry point of these magnitudes so that with inadvertent misalinement of the rocket impulse by as much as $10^\circ$ the vehicle could probably still be landed at a predesignated point.

As an indication of the relative inefficiency of a radial impulse alone as compared with a tangential impulse for accomplishing the transition from orbit to atmosphere (150 miles to 70 miles), it would require a radial velocity of 680 feet per second as compared with a tangential velocity of 150 feet per second to give a reentry angle of $-1/2^\circ$.

## Atmospheric Flight Trajectories

Method of analysis.- As a means of studying the possible trajectories of the satellite configuration after reentry into the earth's atmosphere, the equations of motion for a satellite (for a circular nonrotating earth) were written with the aerodynamic lift and drag forces included. The geometric relationships to be considered after reentry are illustrated in figure 6. The configuration was assumed to have attitude-control capabilities, zero thrust during reentry, and a high drag (flat surface approximately normal to flight path). In addition the resultant force was assumed always to act normal to the surface whenever changes in attitude were made.

Equating the forces (fig. 6(a)) which act along the flight path of the reentry vehicle permits an equation of motion to be written as follows:

$$m\dot{V} = -D - W \sin \gamma \tag{8}$$

This equation can be expanded to

$$\dot{V} = -\frac{C_R \rho V^2 S \sin \alpha}{2m} - \frac{W_e}{m}\left(\frac{R_e}{R_e + h}\right)^2 \sin \gamma \tag{9}$$

Since

$$W = W_e\left(\frac{R_e}{R_e + h}\right)^2$$

Establishing a space reference axis as in figure 6(a) and equating the forces which act normal to the flight path permits an additional equation of motion to be written:

$$mV(\dot{\delta}) = L - W \cos \gamma \tag{10}$$

It is desirable to express this equation in terms of the flight-path angle and the angular travel around the earth $\theta$; thus,

$$mV(\dot{\gamma} - \dot{\theta}) = L - W \cos \gamma \tag{11}$$

where

$$\dot{\theta} = \frac{V}{r} \cos \gamma$$

Equation (11) can be expanded to

$$\dot{\gamma} = \frac{C_R \rho V S \cos \alpha}{2m} - \frac{W_e}{mV}\left(\frac{R_e}{R_e + h}\right)^2 \cos \gamma + \frac{V}{r} \cos \gamma \tag{12}$$

Inasmuch as the incremental changes in the radius $r$ are equal to incremental changes in altitude $h$ (fig. 6(a)), the equation for rate of change of altitude may be written (fig. 6(b))

$$\dot{h} = V \sin \gamma \tag{13}$$

Equations (9) to (13) were used to calculate the trajectories of the reentry vehicle for various initial conditions as it reentered the atmosphere. In order to simplify some of the calculations the variation of atmospheric density with altitude was approximated by the expression

$$\rho = 0.003e^{-Bh} \tag{14}$$

where $B = 1/23{,}000$. This expression gives a good approximation of the density-altitude relationship presented in reference 2 up to about 350,000 feet. A resultant-force coefficient $C_R$ of 1.7 based on modified Newtonian theory was used for all cases that are presented.

The trajectories of the configuration were calculated for conditions of an initial altitude of 350,000 feet, a velocity of about 26,000 feet per second, and at various reentry flight-path angles from $-1/4^{\circ}$ to $-2^{\circ}$. The exact value of initial velocity used for any calculation was that which gave a zero rate of change of flight-path angle (earth radius assumed to be 4,000 miles).

A range of wing loading of from 10 to 30 pounds per square foot was covered. The angle of attack was held constant except in a few cases where it was changed in step increments at a certain point and then maintained constant for the remainder of the calculation. The angle-of-attack range was from $60^{\circ}$ to $90^{\circ}$.

The trajectory calculations were made on a digital computer.

Effect of reentry flight-path angle.- Calculated trajectories which start from different reentry angles are presented in figure 7 as variations of deceleration, velocity, and flight-path angle plotted against altitude. Results are presented for reentry angles of $-1/4^{\circ}$, $-1/2^{\circ}$, $-1^{\circ}$, and $-2^{\circ}$; all results shown are for a wing loading $W/S$ of 20 pounds per square foot for a constant angle of attack of $90^{\circ}$. The variations of deceleration, which are presented in g units, show that the same peak value of 8g is reached for reentry angles $\gamma_o$ of $-1/4^{\circ}$, $-1/2^{\circ}$, and $-1^{\circ}$. Although the flight-path angles are initially different, the plot shows that the flight-path angle and velocity converge to a common relationship as altitude decreases before the deceleration reaches a maximum. Thus, it would be expected that the same maximum deceleration would occur in each of these cases. The results of reference 1 showed that for large reentry angles and accelerations the effects of gravity can be neglected and the maximum deceleration considered a function of the sine of the reentry angle. The present results would be expected to differ from reference 1 in the range of reentry angles of $1^{\circ}$ or less because the decelerations encountered are not large with respect to the gravitational acceleration. For the case of reentry flight-path angle of $-2^{\circ}$, the deceleration peaks at the higher value of about 9g. This case also shows that the flight-path-angle and velocity time histories ultimately converge with the other cases but the convergence occurs below the altitude at which maximum deceleration is reached.

Figure 7 also shows that as the altitude decreases from 350,000 feet to 300,000 feet, very little change is noted in the velocity and flight-path angles from the initial values. This result also applies to the space trajectories discussed in the previous section. Thus, as previously mentioned, the point at which the effect of the atmosphere is initially included in the calculations is not critical in the range of about 50,000 feet from the initial point selected herein (350,000 feet).

Effect of wing loading.- It is expected that the reentry vehicle would have a wing loading somewhere in the range from 20 to 30 pounds per square foot. As a means for determining the effect that different wing loadings might have, trajectories were calculated with wing loadings of 20, 25, and 30 pounds per square foot. Figure 8 shows the variations of deceleration, velocity, and flight-path angle for three cases starting with a reentry angle of $-1^{\circ}$. The one set of curves is used to represent the three cases because the only significant difference in the trajectories was a shift in altitude at which corresponding values of the quantities shown were reached; hence, the three altitude scales are displaced from each other by about 4,600 feet. This shift of the altitude scales is such as to cause the atmospheric densities for a given point on the curves representing the three trajectories to be proportional to the wing loading.

Effect of small lift forces on trajectories.- The deceleration calculated in each of the reentries shown in figures 7 and 8 stayed above 7g for periods of 30 seconds or longer. This deceleration history represents a rather severe loading on the pilot even if he is protected by a "g-suit," and it is desirable to alleviate this condition. If the trajectory were controlled so that the vehicle underwent more of its deceleration in the less dense atmosphere, then the magnitude of the deceleration would be less. Reentering at very low flight-path angles in an attempt to slow down at high altitude is ineffective because, as shown in figure 7, the peak deceleration is not critical to the reentry angle for the range between 0 and $-1^{\circ}$. It becomes necessary then to apply lift forces to the vehicle and a method suggested is to vary the angle of attack from $90^{\circ}$ to less than $90^{\circ}$ so as to direct the resultant force upward from the flight path and thereby obtain a lift component. Reference 3 presents information regarding the effect of lift upon reentry trajectories. Figure 9 shows time histories for two examples in which the angle of attack was varied from $90^{\circ}$ in a step fashion at a certain point during the reentry, and also for an example where the angle of attack was unchanged from $90^{\circ}$ to present a basis for comparison. All of the examples start from a reentry angle of $-1/2^{\circ}$. In one example the angle of attack is changed from $90^{\circ}$ to $80^{\circ}$ when the deceleration reaches 3g. In this case the peak deceleration is about 4.5g, which is a tolerable loading for a pilot protected by a g-suit. Thus, it is apparent that lift forces created in this manner could be an effective way of reducing decelerations. In the other example presented, the angle of attack is changed from $90^{\circ}$ to $60^{\circ}$ when the deceleration builds up to 1 g. In this case the deceleration stays less than 2g but the trajectory exhibits a long-period oscillation. These examples show that angle of attack has a marked effect on deceleration, and it appears likely that a constant deceleration for a considerable part of the trajectories could be obtained by proper programing of angle of attack such as is proposed in reference 4.

The horizontal distances traveled for the examples shown in figure 9 show a wide variation depending upon the angle of attack that was utilized. For the purpose of demonstrating the effect of angle of attack upon the horizontal distance traveled from the initial reentry point, a number of trajectories starting with a reentry angle of $-1^\circ$ were calculated with different angle-of-attack programs. Figure 10 presents the variation of horizontal distance traveled as a function of angle of attack for three different programs of angle of attack. The range reached for the case where the angle of attack was held at $60^\circ$ throughout the trajectory was about 3,700 miles as compared with a range of about 1,400 miles for the case where the angle of attack was kept at $90^\circ$. A comparison of the data for the cases where the angle of attack was $80^\circ$ or less shows that the point in the trajectory at which the angle of attack is changed from $90^\circ$ has a substantial effect upon the distance traveled. The data of figure 10 show that changing the angle of attack from $90^\circ$ to $60^\circ$ at the point where the deceleration reaches 1 g resulted in about 600 miles additional travel over that obtained by changing the angle of attack from $90^\circ$ to $60^\circ$ at the point where the deceleration reaches 3g. Figure 9 shows that the 3g point occurs only 40 seconds after the 1 g point for the case where the angle of attack is maintained at $90^\circ$ throughout the run.

The possibility of displacing the flight path laterally by holding various angles of sideslip (at very high angles of attack, sideslip is created by rolling about the longitudinal body axis) was also studied. Figure 11 shows the variation of lateral distance with distance along the original flight path from the reentry point to the recovery point for values of sideslip $\beta$ of $30^\circ$ and $10^\circ$. In these cases the distance along the original flight path would be obtained by holding the angle of attack constant at various values between $90^\circ$ and $60^\circ$ and the variations shown should not be extrapolated beyond this range of angle of attack. The results show that for distances of about 3,700 miles from the initial point (which can be obtained with an angle of attack of $60^\circ$) the lateral distance would be of the order of 200 miles for $\beta = 10^\circ$ and slightly over 600 miles for $\beta = 30^\circ$. For a reentry with $\alpha$ held at $90^\circ$, the lateral distance traveled would be about 40 miles for $\beta = 10^\circ$ and about 120 miles for $\beta = 30^\circ$. Increasing angle of sideslip also causes a slight increase in the distance traveled along the original flight path because of the reduction of drag brought about by tilting the resultant force away from the flight path.

## STABILITY AND CONTROL

This section describes some of the stability and control aspects for the period of flight from just prior to start of reentry to landing. The discussion is given in a chronological order.

## Orbiting and Retrorocket Phase

During the orbiting phase of flight the pilot would, as previously mentioned, use reaction controls. These controls would be similar to those proposed for an advanced research airplane and would provide maximum angular accelerations on the order of $5^{\circ}/sec^2$ in roll and $3^{\circ}/sec^2$ in pitch and yaw. The pilot would be required to do very little controlling during this phase but no doubt he would want to control the airplane attitude, for example, to observe the earth. Immediately prior to firing the retrorocket the pilot would be required to aline the airplane so that the retrorocket thrust axis is approximately alined with the airplane flight path. The thrust axis of the retrorocket should be alined as closely as possible with the airplane center of gravity so as to minimize the pilot's control task when the retrorocket is burning. Furthermore, the thrust of the retrorocket should be of such a magnitude that any moments arising from thrust misalinement can be balanced by the low thrust-reaction controls. Upon burnout of the retrorocket the pilot would use the reaction controls to pitch the airplane to an angle of attack of about $90^{\circ}$ for the reentry phase.

## Reentry Phase

During the reentry phase of flight the pilot would be required to maintain an angle of attack in a range from about $60^{\circ}$ to $90^{\circ}$ and also he would be required to maintain the roll and yaw angles as desired.

Longitudinal stability and control.- The airplane should be designed to have positive static longitudinal stability in the reentry configuration. This stability can be provided by locating the center of gravity very near the centroid of area and making the under side of the wing convex. The amount of curvature will probably be dictated by aerodynamic-heating considerations. The static stability should be small in magnitude because it will be difficult to provide a longitudinal control having very high effectiveness. The aerodynamic data available for reentry shapes indicate that maintenance of a small static margin will be possible. The longitudinal control at $90^{\circ}$ angle of attack might be obtained by control surfaces hinged at the edge of the wing in a manner similar to that sketched in figure 1.

In connection with the reentry phase, studies are needed to determine the kind of information that needs to be provided to the pilot to enable him to keep the airplane in the desired attitude and on the desired flight path. The required information could be in the form of a completely visual display or it could be a ground-control-approach type of operation with the pilot receiving verbal instructions from ground stations. Also it should be noted that the pilot's control techniques during

reentry are in some cases different from usual. For example, when flying in the 90° angle-of-attack condition, the pilot, in order to make a pullup, must reduce the angle of attack so as to tilt the resultant-force vector upward from the existing flight path.

Lateral stability and control.- Unlike conventional airplane, the reentry configuration can be made to have static stability in roll about the body axis while flying in the 90° angle-of-attack condition. This roll stability can be obtained by incorporating convex curvature on the under side of the wing.

At 90° angle of attack the reentry configuration will have low or neutral static directional stability about the body axis, and the pilot must keep the airplane properly alined; however, he would not require a highly effective control. Roll and yaw control could probably be obtained with control surfaces hinged at the leading and trailing edge of the wing such as is shown in the sketch of figure 1. In order to avoid cross control moments the controls may have to be used differentially or in combination.

Although much additional study and experiment are needed concerning the stability and control characteristics of the reentry configuration, the concept appears reasonable from a stability and control standpoint. Upon completion of the reentry phase (aerodynamic heating negligible and dynamic pressure sufficient to maintain flight) the transition to the gliding phase is made. This will normally be acomplished at low supersonic or at subsonic speeds.

## Gliding Phase

The transition to the gliding phase of the flight could be made by unfolding the outer wing panels into the wing panel or by some other variable geometry feature. Because these wing panels are located rearward of the airplane center of gravity they will provide a negative pitching moment and reduce the angle-of-attack range used for gliding flight. A critical condition from the directional stability standpoint may occur when the transition is made from the large angle of attack to the relatively low angle of attack because of the probability of any vertical stabilizer being effectively blocked. For gliding flight the control system could be the conventional arrangement for a delta-wing airplane configuration.

## Approach and Landing

It is assumed, as a starting point in assessing the approach and landing behavior of the reentry vehicle, that the angle of attack of the

aircraft has just been reduced from the reentry value of 90° and that this event occurs at an altitude of 125,000 feet and a velocity of 2,000 feet per second. Assuming that a wing loading of about 15 pounds per square foot is a reasonable value for the configuration during this phase, calculations were made of the pull out and glide capabilities. At this altitude and velocity the lift coefficient for steady flight is beyond the capabilities of the aircraft so that a glide pull out is begun at a high lift coefficient ($C_L = 0.75$) and ends at an altitude of 92,500 feet and a velocity of 1,800 feet per second so that a distance of 20 miles is covered. Using a lift-drag ratio of 4 for supersonic speeds and 11 for subsonic speeds it is estimated that the configuration could cover approximately 200 miles straight ahead or about 150 miles if a 180° turn must be made in order to head toward a desired landing area. An altitude of 10,000 feet over the landing field was assumed in order to allow for a landing approach. With a $C_L$ of 0.6 and an angle of attack of 16°, touchdown could be at about 90 knots which would allow a rather short ground run.

As pointed out in the discussion of the operational concept, the normal landing would be at a preselected airport not too far to either side of the extended satellite flight path. If, however, some unexpected error were made in the flight path or the ground control, a landing could be made on any 5,000-foot runway within 150 miles of the recovery point. Within the continental limits of the United States there is no spot that is not within 125 miles of an airport having 5,000-foot runways. It is practically impossible therefore for the aircraft to be out of range of a suitable emergency field at the time of recovery providing that weather conditions are not unfavorable.

## HEAT-TRANSFER RATES

Heat-transfer rates on the lower surface of the reentry vehicle at angles of attack of 90° were calculated on the basis of some simplifying assumptions. These assumptions were necessary because information was not available on pressure distribution, skin friction, or heat transfer on the lower surface of a low-aspect-ratio wing at an angle of attack near 90° in hypersonic flow. Use was therefore made of some information available on pressure gradients and heat transfer on flat disks, flat-faced cylindrical bodies, and bodies with a hemispherical nose.

In order to compute the heat-transfer rate on the lower surface of the wing of the assumed research vehicle, the wing was assumed to be equivalent to a circular disk of the same area as the wing. Heat-transfer rates were then computed for the stagnation point of a hemispherical nose having a diameter equal to the diameter of the equivalent disk. The heat-transfer rate for the disk was then taken as half of that for the hemispherical nose. Because of the convex curvature of the lower surface of

the wing, the heat-transfer rate near the stagnation point is expected to be higher than that for a flat surface but lower than that for a hemisphere. Near the edges the heat transfer would be lower than that for a flat-faced surface but higher than that for a hemisphere. The average heat-transfer rate across the lower surface of the wing was therefore arbitrarily taken as 25 percent greater than for the stagnation point of the flat-faced disk. The heat transfer to the upper surface of the wing for all angle-of-attack conditions was assumed to be negligible.

The heat-transfer rates at the stagnation point of a hemispherical nose were computed first by the method of Fay and Riddell (ref. 5) by making use of ideal gas properties. During the process of computing heat-transfer rates the method of Romig (ref. 6) was tried and found to agree closely with that of Fay and Riddell for the conditions encountered in the trajectories of the assumed vehicle. Since Romig's method required less computing time, it was used for all of the subsequent calculations. For the stagnation point of a hemispherical nose, Romig gives the relation for heat-transfer rate as

$$q = 0.0145 M_\infty^{3.1} \sqrt{\frac{P_\infty}{R_N}} \tag{15}$$

where

$q$ heat-transfer rate in Btu/sec-sq ft

$M_\infty$ free-stream Mach number

$P_\infty$ free-stream pressure, lb/sq ft

$R_N$ radius of the hemisphere, ft

For a flat circular disk the heat-transfer rate would be

$$q = 0.00725 M_\infty^{3.1} \sqrt{\frac{P_\infty}{R_N}} \tag{16}$$

Increasing this rate by approximately 25 percent to account for curvature on the lower surface of the wing, the heat-transfer rate is then

$$q = 0.00905 M_\infty^{3.1} \sqrt{\frac{P_\infty}{R_N}} \tag{17}$$

If $R_N$ is taken as 8 feet on the basis of preliminary estimates of a reasonable value, equation (17) reduces to

$$q = 0.0032M_\infty^{3.1}\sqrt{P_\infty} \tag{18}$$

The heat-transfer equation (eq. (15)) was developed by Romig for the condition where the wall temperature was equal to the free-stream temperature. This simplifying assumption is commonly made in calculating heat-transfer rates and is justified because the temperatures encountered behind the normal shock during the reentry trajectories are large compared with allowable wall temperatures. It should be noted that the heat-transfer rate as given by equation (18) assumes that the flow is laminar over the disk. This assumption appears to be justified by the fact that the Reynolds number, based on free-stream conditions and a radius of 8 feet, is of the order of 100,000 near the time in a trajectory when the laminar heat-transfer rate is maximum.

The Mach number $M_\infty$ in a trajectory was computed from the vehicle velocity and the altitude time histories such as that presented in figure 9 and the temperature-geometric altitude relationship as given in reference 2. Pressure $P_\infty$ was computed by using the temperature-altitude relationship in reference 2 and the following relation for density

$$\rho_\infty = 0.003e^{-\frac{h}{23,000}}$$

from which the relation for pressure is

$$P_\infty = 0.003RTe^{-\frac{h}{23,000}}$$

The results of the computations of heat-transfer rates for various conditions of reentry angle $\gamma_o$, angle of attack $\alpha$, and wing loading $W/S$ are presented in figures 12 to 17. The effect of reentry angle on heat-transfer rate is shown in figure 12 for $\alpha = 90^\circ$ and $W/S = 20$ pounds per square foot. The maximum heat-transfer rate is about the same for reentry angles of $-1/4^\circ$, $-1/2^\circ$, and $-1^\circ$ but about 20 percent greater for reentry angle of $-2^\circ$. The total heat input (integral of heating rate), however, decreases with increase in the reentry angle. Comparison of the time histories of the heat-transfer rates with corresponding time histories of deceleration along the flight path showed that the maximum heating rates occurred appreciably before maximum deceleration. For example, compare the time history of heat-transfer rate for the case of

$\gamma_o = -1/2^o$ shown in figure 12 with the time history of deceleration for the same case as shown in figure 9.

The effect of changing angle of attack during the trajectory on the heating rate is illustrated in figure 13 for $\gamma_o = -1/2^o$ and W/S = 20 pounds per square foot and in figure 14 for $\gamma_o = -1^o$ and W/S = 25 pounds per square foot. The angle-of-attack conditions are as follows. For $\alpha = 90^o$, this angle of attack was maintained throughout the trajectory. For $\alpha = 80^o$ at 3g, the angle of attack was initially $90^o$ and changed to $80^o$ when a deceleration of 3g along the flight path was attained. For $\alpha = 60^o$ at 1 g, the angle of attack was initially $90^o$ and changed to $60^o$ when a deceleration of 1 g was reached. For the $\alpha = 60^o$ case, the angle of attack was maintained at $60^o$ throughout the trajectory. The heat-transfer rates computed for angles of attack other than $90^o$ are questionable since the method is derived for the $90^o$ angle of attack only. If the flow pattern and the position of the stagnation point change appreciably with change in angle of attack from $90^o$, the computed heating rates may be expected to be in error and it is probable that the heat-transfer rate will be appreciably higher toward the leading edge. If the flow change for the $80^o$ angle-of-attack case is assumed to be negligible, it may be seen that changing from $\alpha = 90^o$ to $\alpha = 80^o$ at a time when the deceleration reaches 3g results in no change in the maximum heating rate and only a slight change in the total heat input. This maneuver (changing from $\alpha = 90^o$ to $80^o$) was shown in the section on the discussion of trajectories to result in an appreciable reduction in maximum deceleration $\left(8g \text{ to } 4\frac{1}{2}g\right)$.

The effect of increasing the weight of the research vehicle on the heat-transfer rates is shown in figure 15 for $\gamma_o = -1^o$ and in figure 16 for $\gamma_o = -1/2^o$. Increasing the weight by 50 percent and thereby increasing the wing loading from 20 to 30 pounds per square foot increases the maximum heating rate by about 20 percent.

Some heat-transfer rates were computed for $\alpha = 43^o$, a condition which would give an attached shock on a wedge at Mach numbers greater than about 7. The mean chord station was selected for purposes of the computations. The laminar heat-transfer rate was first computed at a distance of 1 foot from the leading edge on the lower surface on the basis of local flow conditions behind the attached shock. The relations between heat transfer and Reynolds number of reference 7 were utilized for computing the heat transfer in laminar flow. The heat-transfer rate at other positions along the chord were then taken as inversely proportional to the square root of the distance from the leading edge. The average heat-transfer rate over the leading edge was computed and corrected for sweep angle on the assumption that the leading edge was

approximated by a half-cylinder having the same radius as the leading edge. The heat-transfer rate averaged over the mean chord and the average rate at the leading edge for a reentry angle $\gamma_o$ of $-2^\circ$, a wing loading of 20 pounds per square foot, and an angle of attack of $43^\circ$ throughout the trajectory are presented in figure 17. Although the heat-transfer rate as computed by equation (18) loses its significance for the attached-shock case, this calculated curve is presented in figure 17 as a matter of interest. The oscillations of heat-transfer rate are due to the relatively high lift associated with the $43^\circ$ angle of attack, which causes a skipping motion of the vehicle. The average heat-transfer rate over the leading edge for $\alpha = 43^\circ$ is appreciably greater than the maximum rates for angles of attack at $90^\circ$ (fig. 12). Furthermore, the average heat-transfer rate at the leading edge at wing stations near the tip may be in the neighborhood of 80 percent higher than those shown in figure 17 because of the smaller leading-edge radius. Angles of attack of $90^\circ$ or approaching $90^\circ$ would therefore appear to offer a more uniform distribution of heat-transfer rates than angles of attack of $43^\circ$ or less.

## HEAT PROTECTION

In order to maintain reasonable weights for a vehicle adapted to the proposed reentry concept, special consideration has to be given to the materials and structure to be used in the basic wing and aerodynamic control surfaces that are exposed to the high heat-transfer rates discussed in the previous section.

René 41 and beryllium are suggested as one possible combination of materials for these structures. The selection of Rene 41 was based on its high ratio of strength to weight at temperatures up to $1,600^\circ$ F. Beryllium was selected on the basis of its high specific heat. The combination of René 41 and beryllium produces a relatively light structure, inasmuch as only 1 pound per square foot of beryllium is required in the lower surfaces to keep the temperature during the peak heat-input period below $1,600^\circ$ F. At $1,600^\circ$ F a large portion of the heat input is reradiated back to the atmosphere. A combination of heat-sink and heat-radiation capability is desirable because it allows reentries to be made at either low reentry angles, where the heat-transfer rates are moderate and the total heat inputs are large, or at higher reentry angles, where the heat-transfer rates are higher but the total heat inputs are lower.

Figure 18 shows the time history of the temperatures of the top and bottom surfaces of the basic wing structure, the heat input, and the heat radiated to the atmosphere by the top and bottom surfaces. The heat-transfer rate is for the reentry configuration with $W/S = 20$ pounds per square foot, $\alpha = 90^\circ$, and $\gamma_o = -1/2^\circ$ shown in figure 9. This reentry

is considered the most severe on the structure from consideration of the heating. Although other reentries apply more total heat to the structure, the radiation of the structure is sufficient to keep the temperature below 1,600° F.

The temperatures of the surfaces were determined by considering the relations of the total heat input, the radiation between the surfaces and to the atmosphere, and the heat absorbed by the René 41 and beryllium material. An emissivity factor of 0.8 was assumed for the radiation of all the surfaces.

The large temperature gradient through the structure would require special consideration of the interconnecting structure to allow for the differences in thermal expansion between the top and bottom sandwich structure. The temperature gradient across the bottom sandwich structure is not expected to create a problem, because of the high conductivity of the beryllium.

Other materials could be used for the structure and heat protection of the reentry vehicle, but it is expected that the resultant weights will be of the same order as the beryllium and René 41 selection.

The theoretical work reported in reference 8 has indicated that ablative materials show promise of being effective as heat shields; however, no experimental data are available for the heat-transfer-rate conditions shown in figures 12 to 16.

Insulated, lightweight, high-temperature heat radiators are also possible for reentry vehicles. If such a radiator were used on the bottom wing surface in the presence of the heat inputs shown in figure 18, essentially all of the heat input would be radiated back to the atmosphere. The maximum surface temperature for such a structure would be about 2,100° F. Attaching this radiating surface to the reentry vehicle and insulating between the structure and surface present problems beyond the scope of this investigation.

## CONCLUDING REMARKS

A concept for a manned-satellite reentry which terminates with a glide type of landing has been described. The results of studies relating to various phases of the reentry are presented and point up the feasibility of the concept. The results show that the retrorocket fired with impulse inaccuracies of about ±2 percent and alinement inaccuracies of about ±10° will produce the desired flight-path angle within 0.04° and the desired location of the reentry point within 600 miles for a -1° reentry angle.

Reentries at 90° angle of attack (nonlifting) starting with flight-path angles between 0° and -1° resulted in peak decelerations of 8g; however, small lift forces obtained by varying the angle of attack between 90° and 60° were effective in lowering the deceleration to about 4g or less. These lift forces were also an effective means of extending the range covered during the atmospheric phase of the reentry and could be a means of compensating for errors in the location of the reentry point caused by errors in the retrorocket-firing maneuver.

## RECOMMENDATIONS

The navigational and control procedures to be used with the reentry vehicle between the reentry and landing points were not determined and present a fruitful field for future research. There are, in addition, many problems associated with the configuration and the operational concept that require further investigation and study. These aerodynamic problem areas are listed as follows:

Low-speed range (Mach numbers to 0.5):

(1) Size of folding panels needed for stability

(2) Study of pitch-up characteristics

(3) Effect of center- and tip-located vertical tails

(4) Comparison of elevons with all-movable surfaces

(5) Relative merits of subsonic and supersonic gliding configurations

Range for Mach numbers from 0.5 to 2.0:

(1) Transition from high angle of attack to low angle of attack due to unfolding panels

(2) Directional stability - determine maximum Mach number for transition

Hypersonic speed range (Mach numbers 6 to 25):

(1) Lift-curve slope at high angles of attack

(2) Stability in pitch and roll

(3) Effectiveness and shift in aerodynamic center due to tab-type controls

(4) Control interactions

(5) Aerodynamic heating - effects of angle of attack and possibility of local hot spots

(6) Aerodynamic heating of shapes similar to that of the proposed configuration

Problems regarding the launching have not been considered, although the problem of emergency escape from an aborted launch may require a somewhat different launch trajectory than an unmanned orbital vehicle. It is possible that the last-stage rocket could be used as a means of propelling the configuration to altitude and velocity conditions from which a controlled emergency landing could be made.

Langley Research Center,
National Aeronautics and Space Administration,
Langley Field, Va., January 7, 1959.

## REFERENCES

1. Allen, H. Julian, and Eggers, A. J., Jr.: A Study of the Motion and Aerodynamic Heating of Missiles Entering the Earth's Atmosphere at High Supersonic Speeds. NACA TN 4047, 1957.

2. Minzner, R. A., and Ripley, W. S.: The ARDC Model Atmosphere. Air Force Surveys in Geophysics No. 86 (AFCRC TN-56-204), Geophysics Res. Div., AF Cambridge Res. Center (Bedford, Mass.), Dec. 1956. (Available as ASTIA Doc. 110233.)

3. Chapman, Dean R.: An Approximate Analytical Method for Studying Entry Into Planetary Atmospheres. NACA TN 4276, 1958.

4. Eggleston, John M., and Young, John W.: Trajectory Control for Vehicles Entering the Earth's Atmosphere at Small Flight-Path Angles. NASA MEMO 1-19-59L, 1959.

5. Fay, J. A., and Riddell, F. R.: Theory of Stagnation Point Heat Transfer in Dissociated Air. Jour. Aero. Sci., vol. 25, no. 2, Feb. 1958, pp. 83-85, 121.

6. Romig, Mary F.: Stagnation Point Heat Transfer for Hypersonic Flow. Jet Propulsion (Technical Notes), vol. 26, no. 12, Dec. 1956, pp. 1098-1101.

7. Van Driest, E. R.: Investigation of Laminar Boundary Layer in Compressible Fluids Using the Crocco Method. NACA TN 2597, 1952.

8. Roberts, Leonard: A Theoretical Study of Stagnation-Point Ablation. NACA TN 4392, 1958.

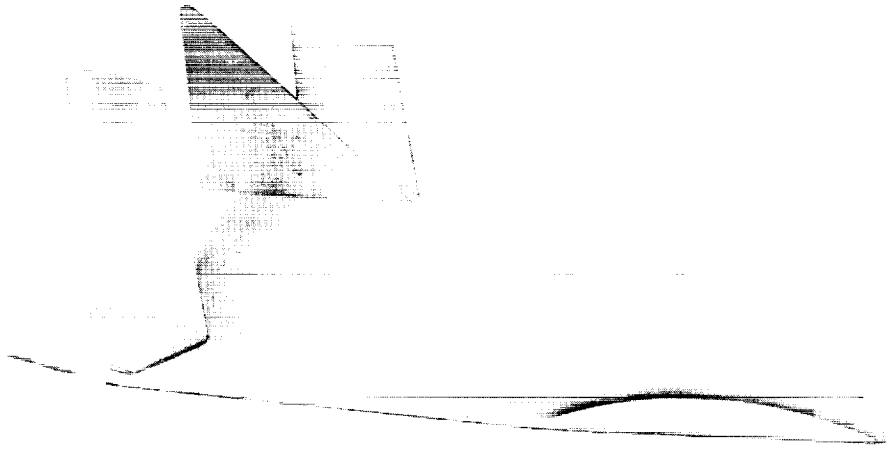

(a) Reentry

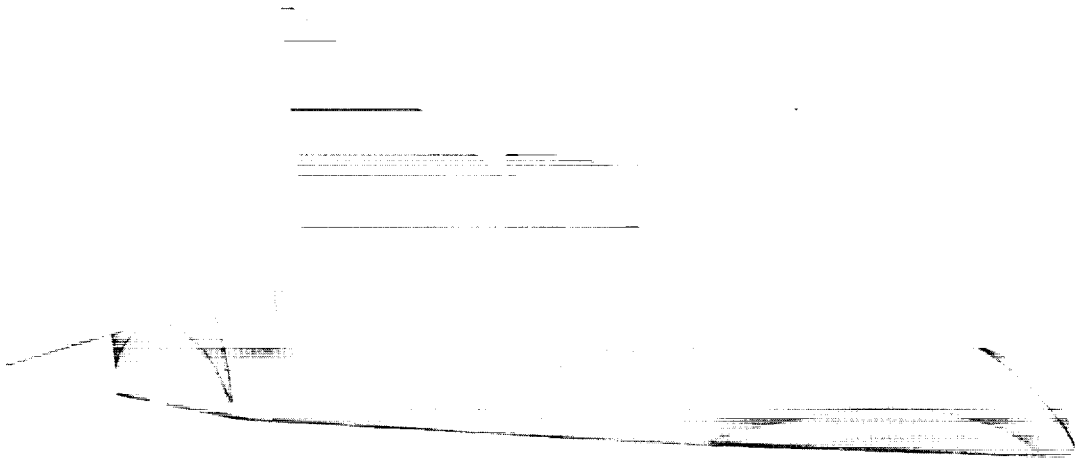

(b) Landing

Figure 1.- Possible reentry configuration.

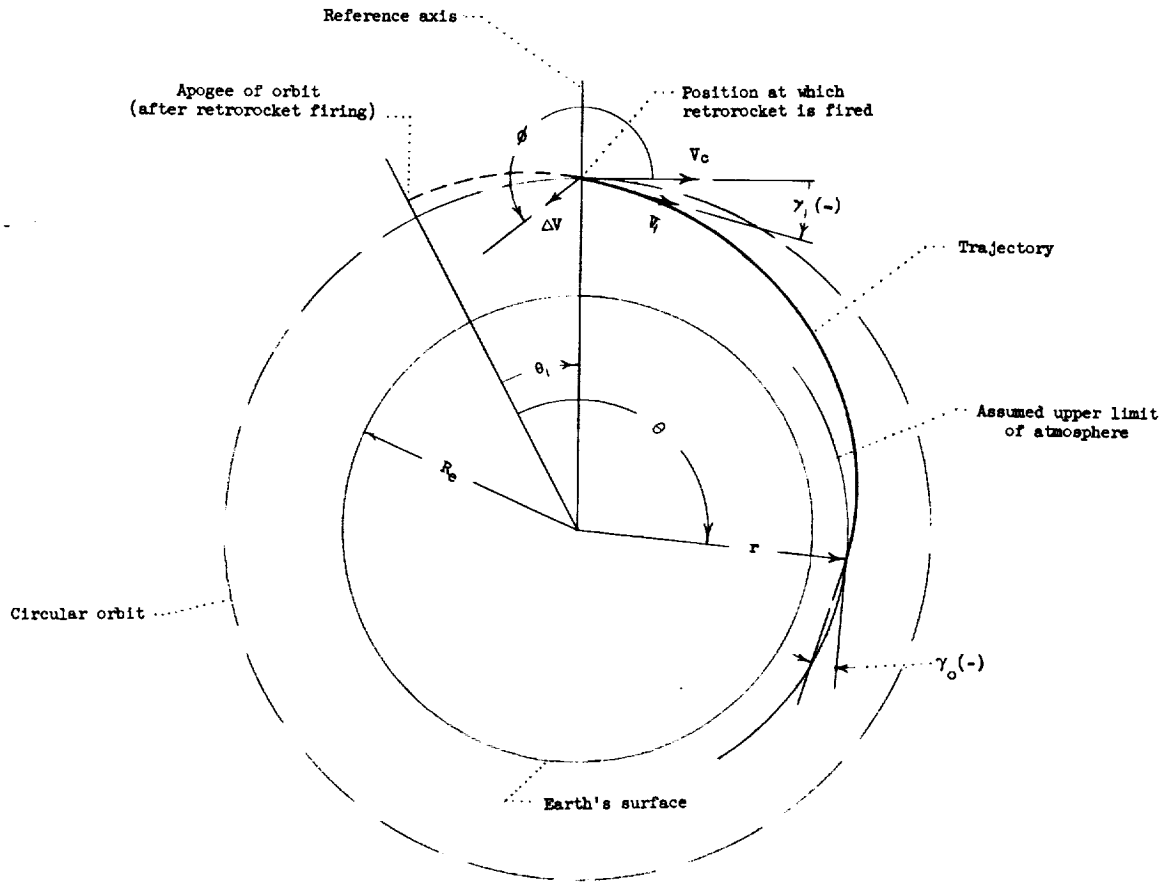


Figure 2.- Diagram of extra-atmospheric phase of reentry.

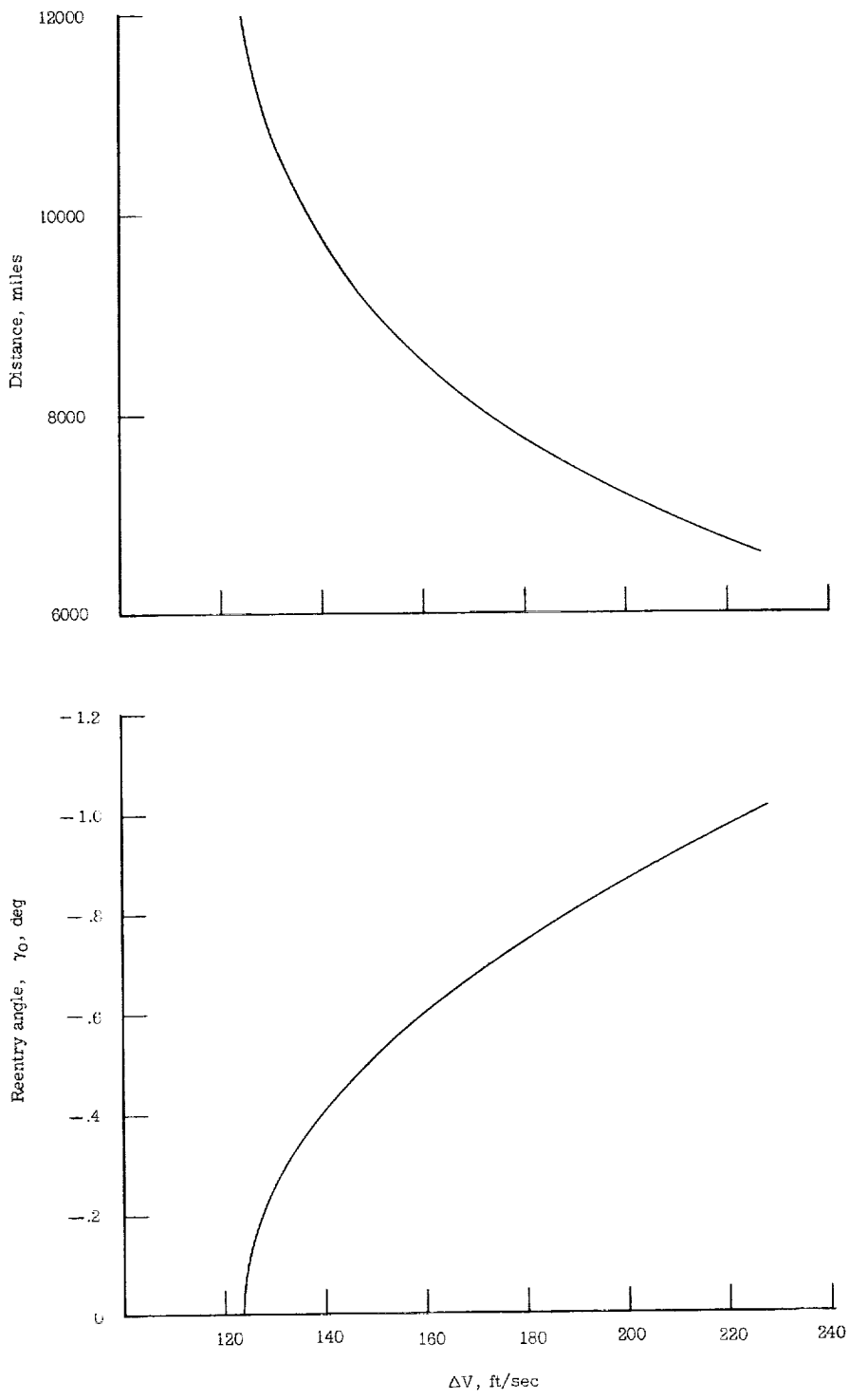


Figure 3.- Effect of retrorocket impulse on reentry angle at 70-mile height and on distance to reentry point.

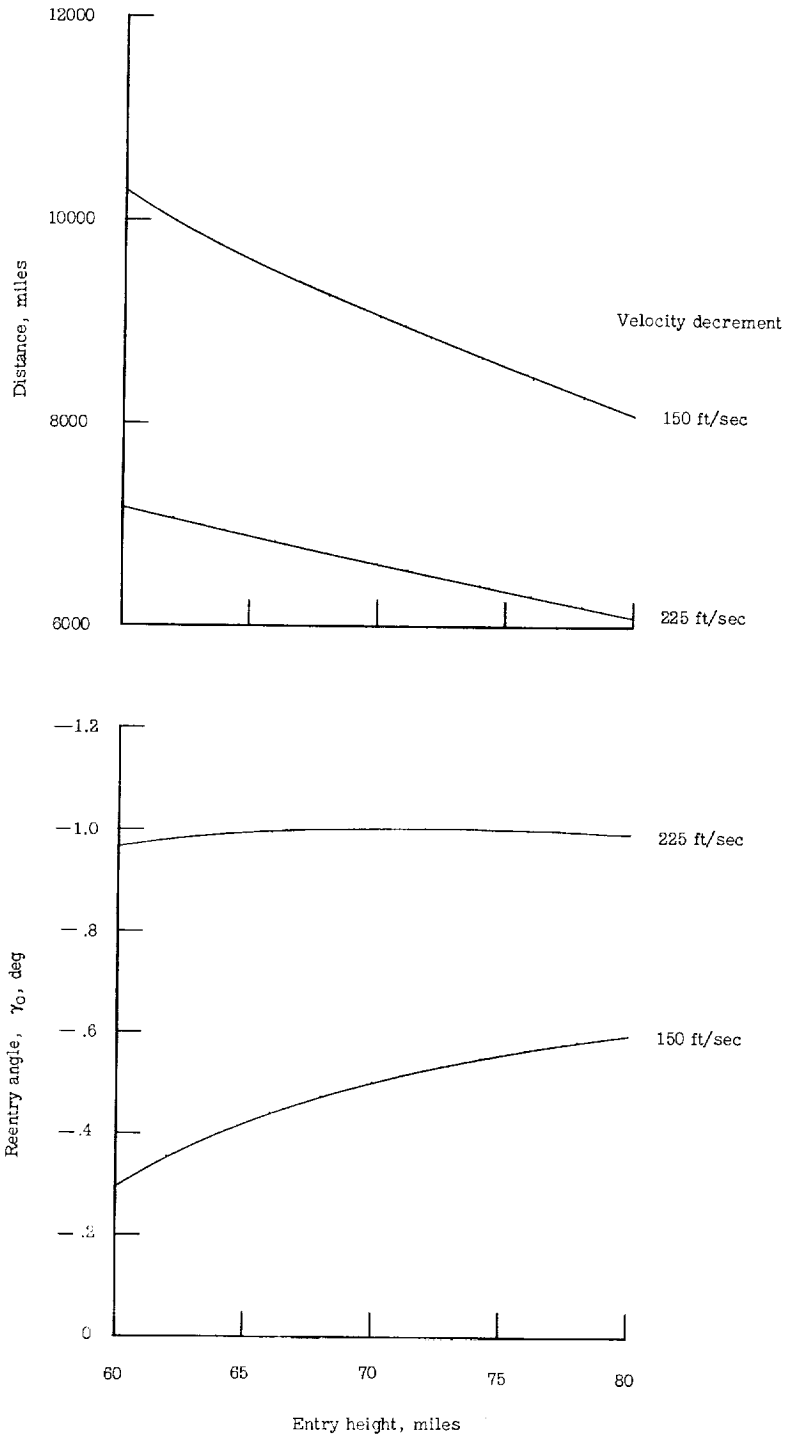


Figure 4.- Effect of height upon reentry angle and distance from retro-rocket firing point to reentry point.

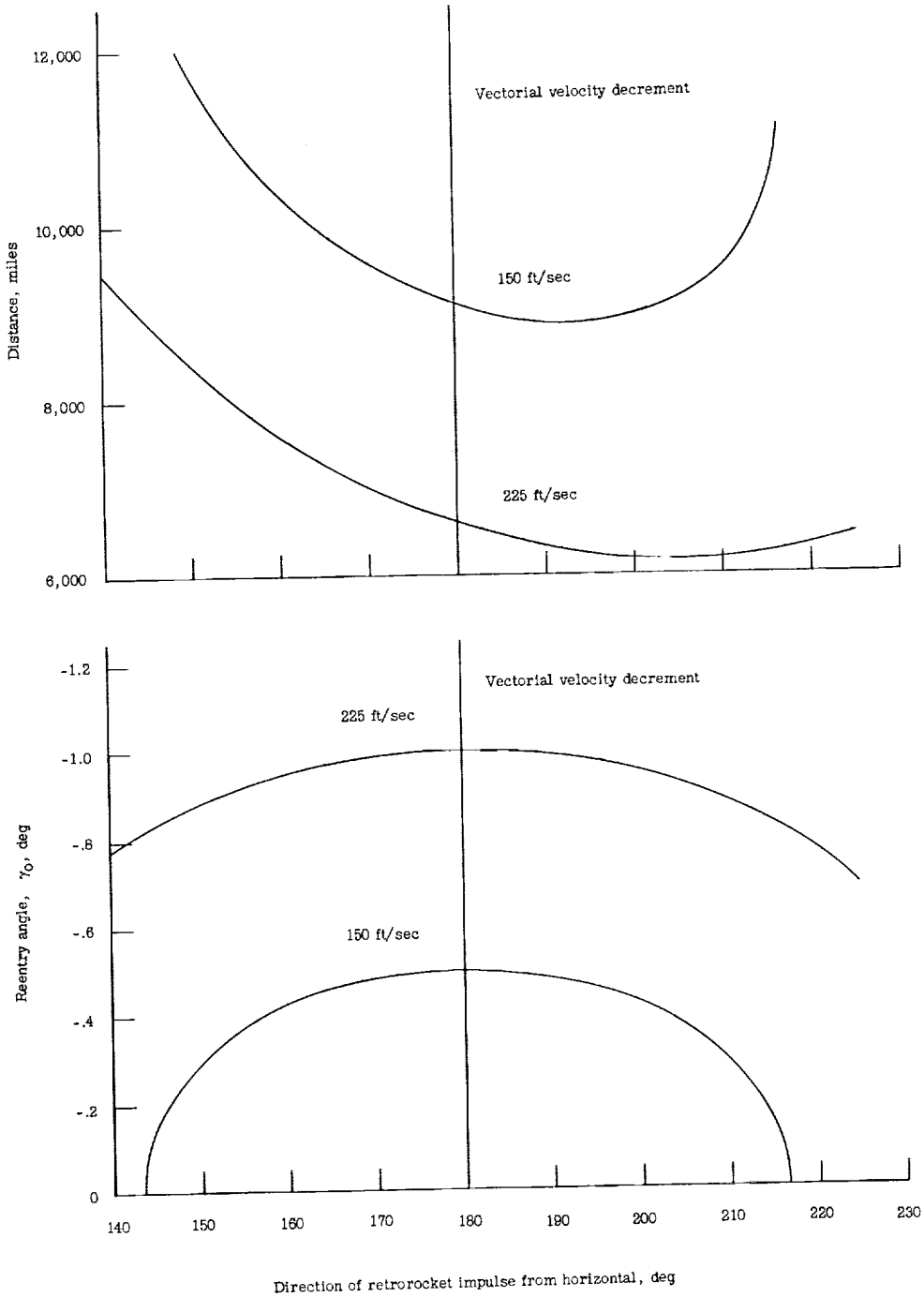


Figure 5.- Effect of variation of alinement of retrorocket impulse in orbit plane on reentry angle and distance from retrorocket firing point to reentry point. Reentry altitude = 70 miles.

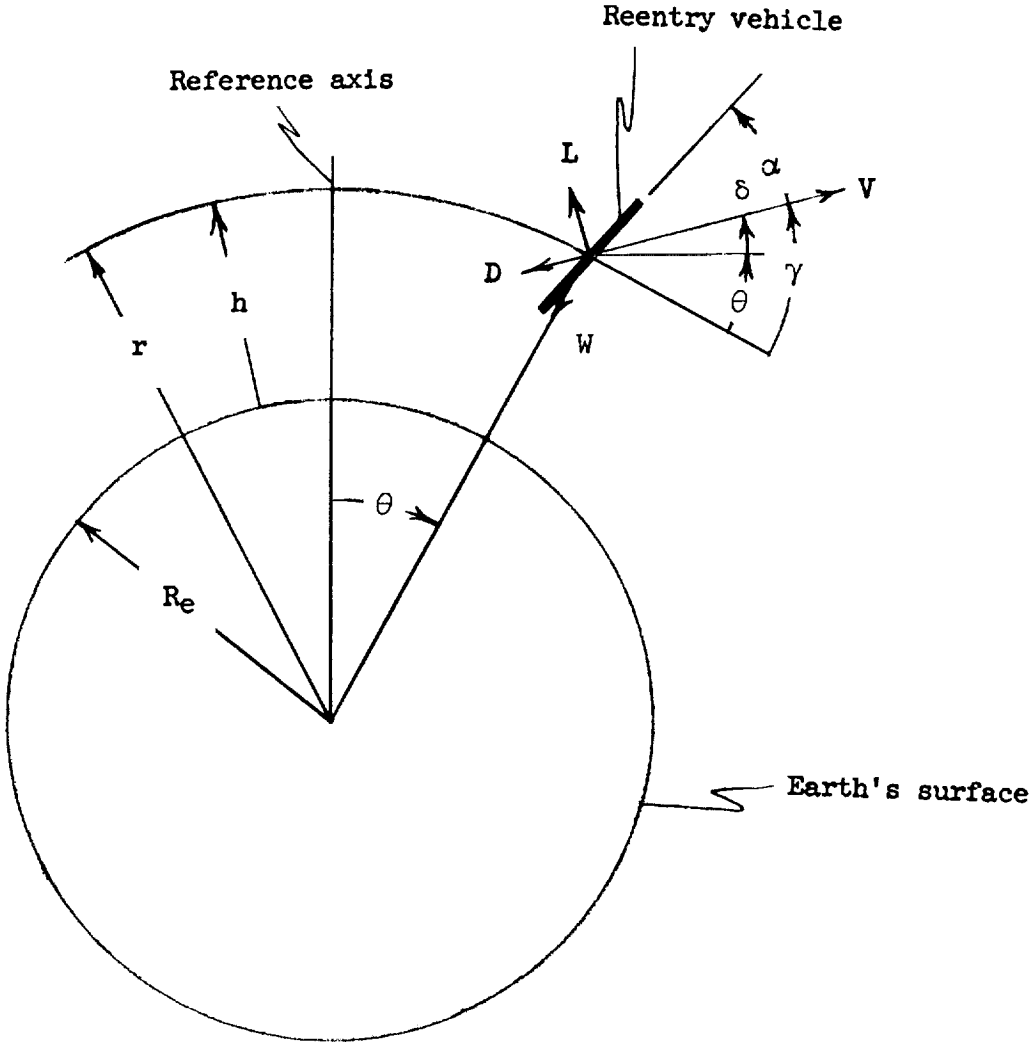


(a) Sketch showing positive direction of forces and angles.

Figure 6.- Generalized diagram of geometrical relationship for intra-atmospheric trajectories.

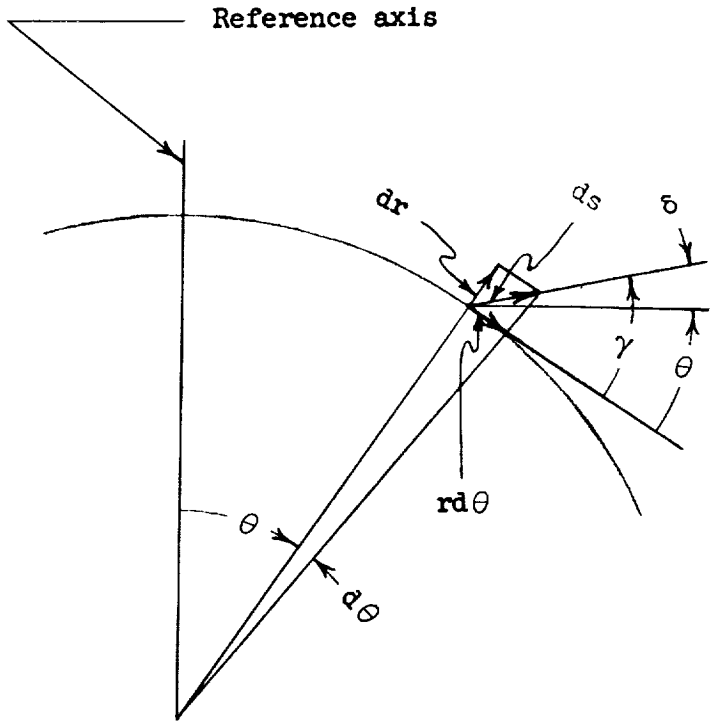


(b) Sketch showing incremental changes in radius and orbit angle with incremental change in distance traveled along the flight path.

Figure 6.- Concluded.

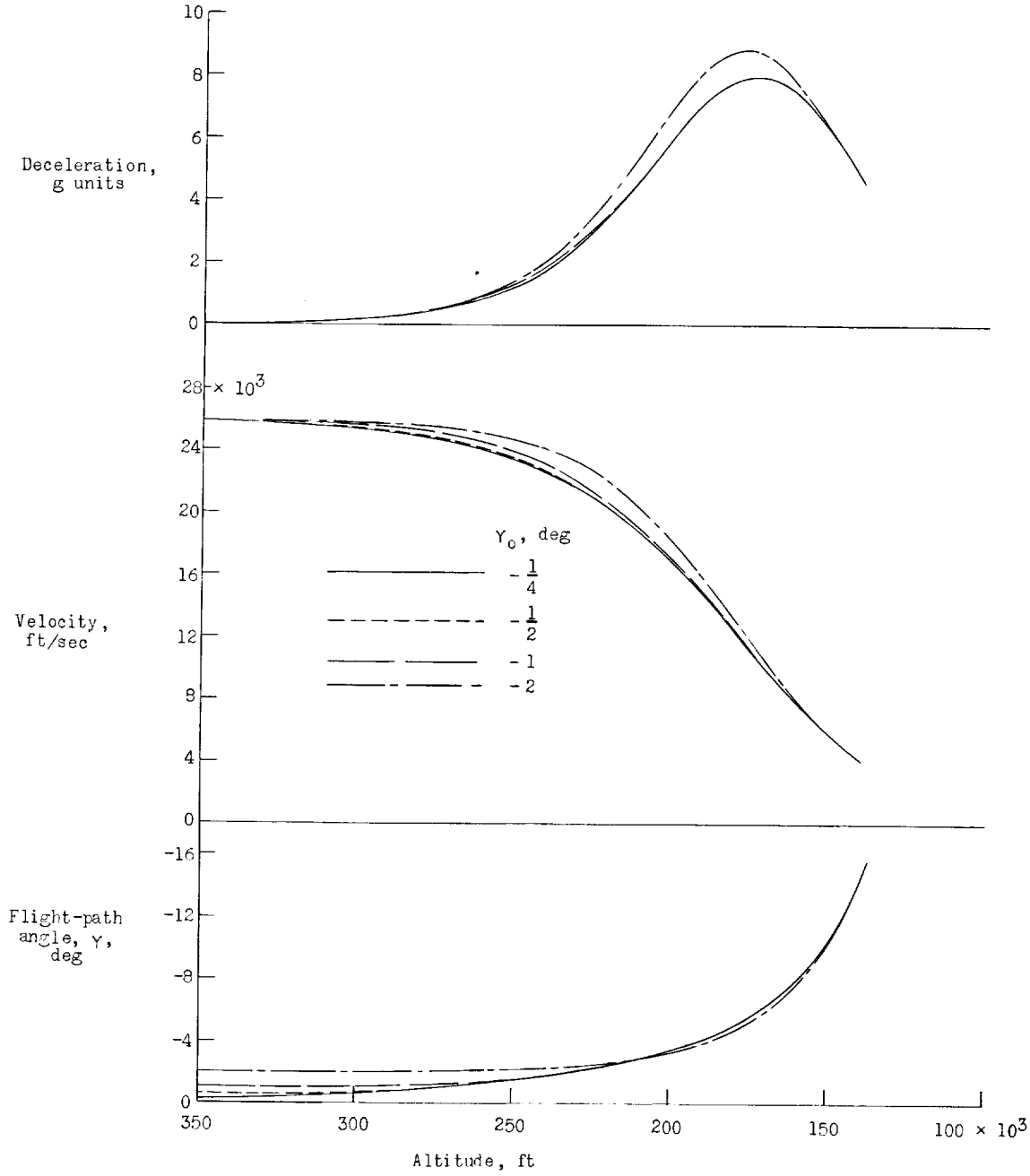


Figure 7.- Effect of reentry angle on the variations of deceleration, velocity, and flight-path angle with altitude. W/S = 20 pounds per square foot; $\alpha = 90^{\circ}$.

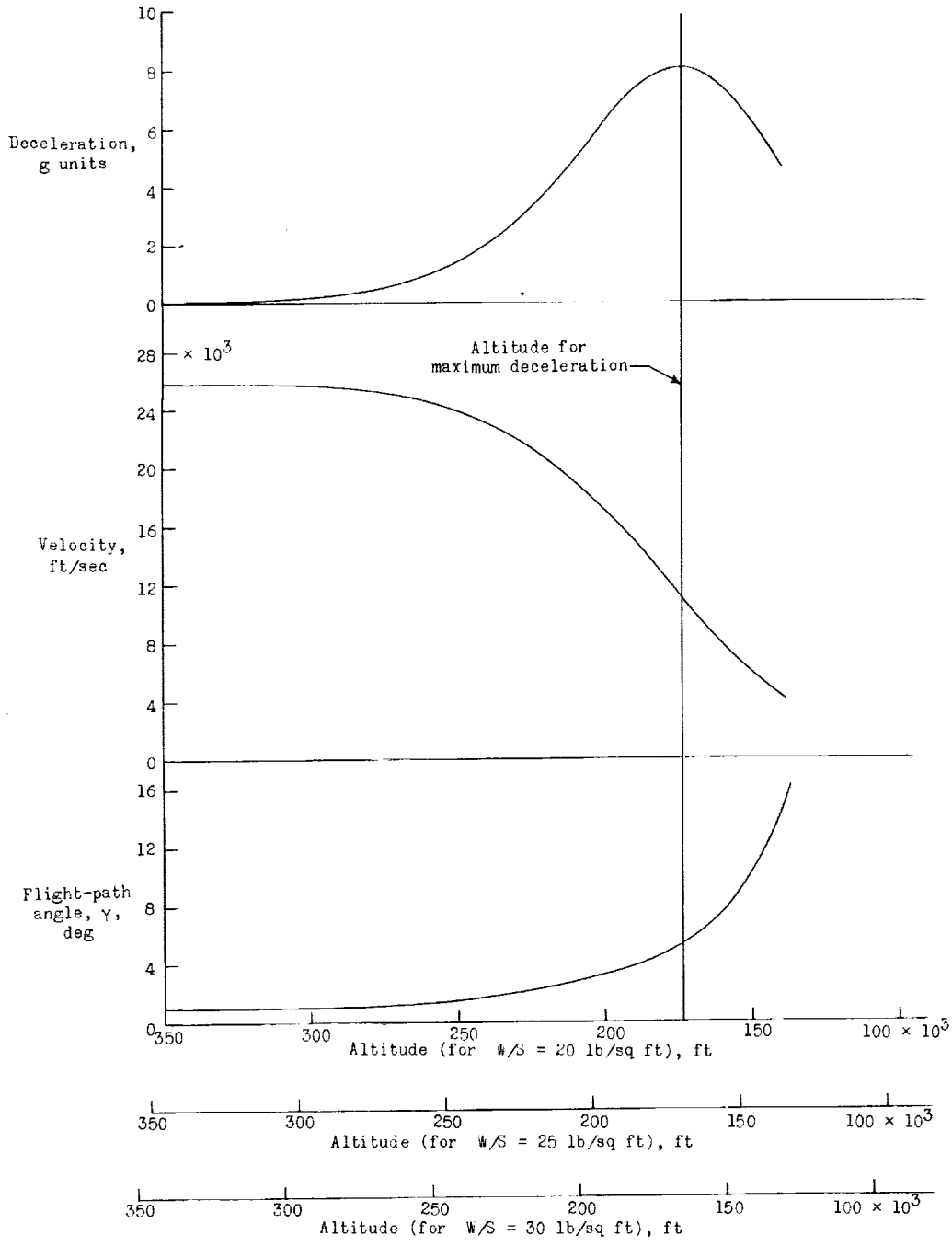


Figure 8.- Effect of wing loading W/S upon the variation of deceleration, velocity, and flight-path angle with altitude. $\gamma_o = -1^o$; $\alpha = 90^o$.

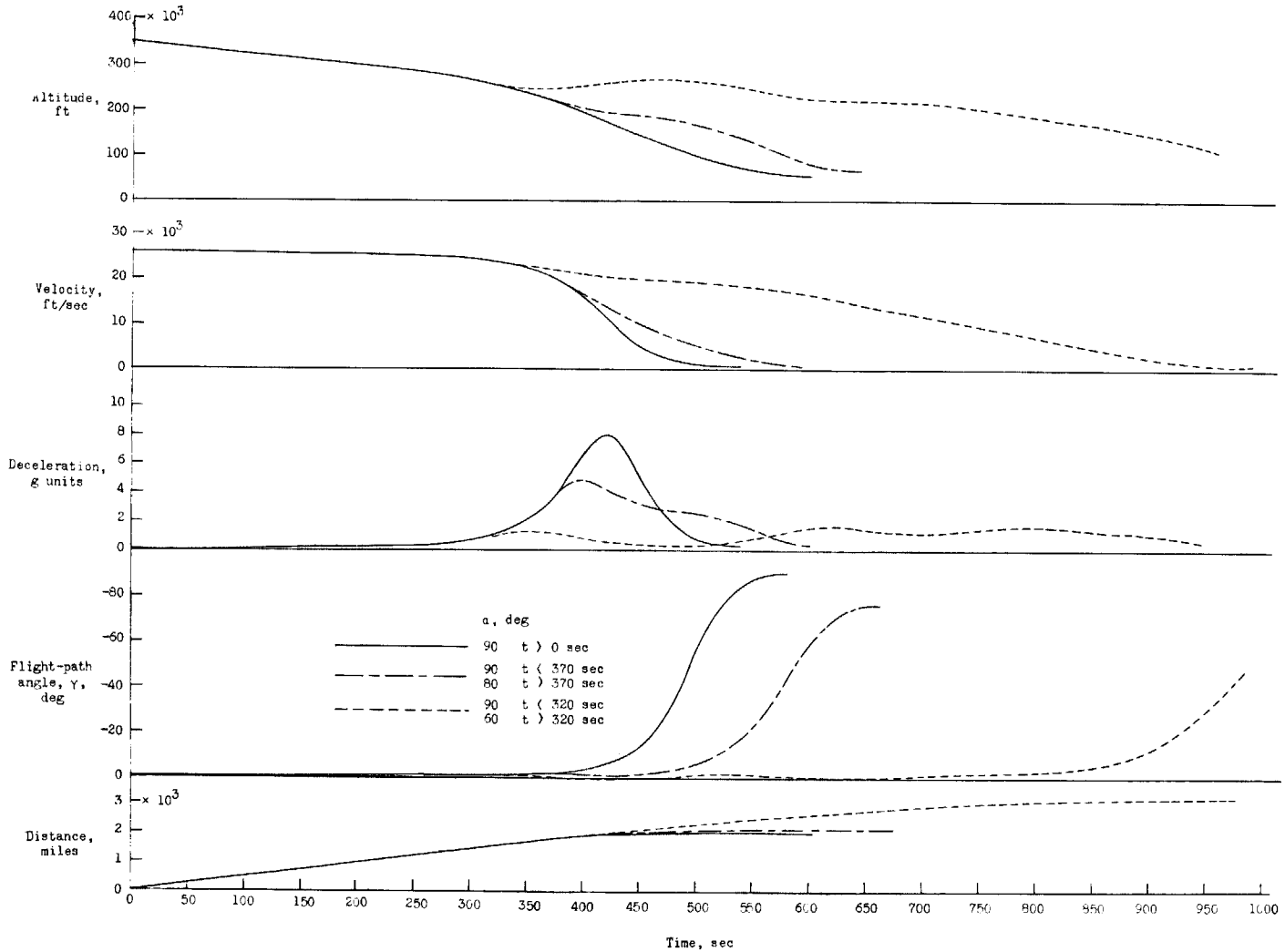


Figure 9.- Time histories showing the effect of various angle-of-attack programs on the deceleration and other trajectory variables. $\gamma_o = -1/2^o$; W/S = 20 pounds per square foot.

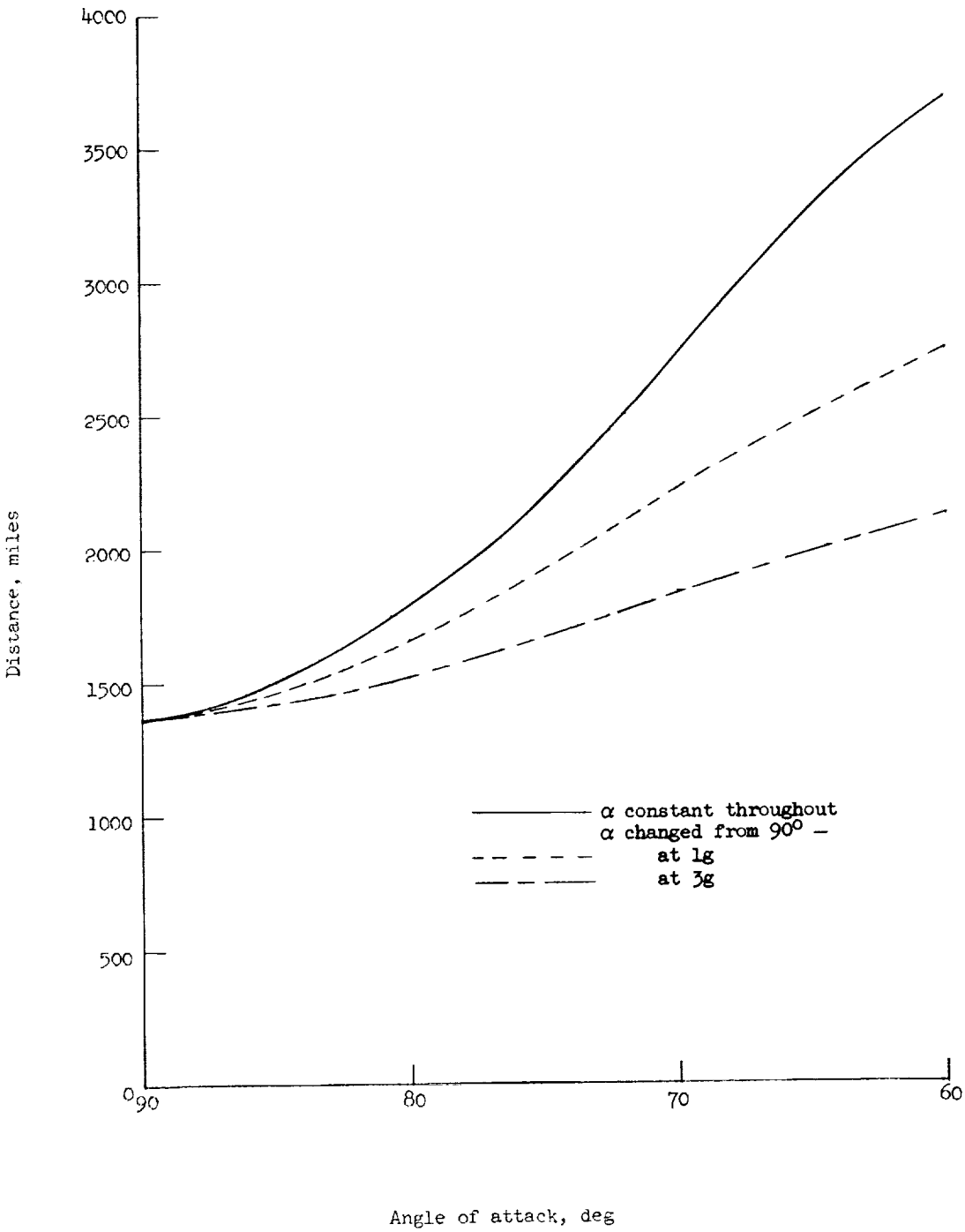


Figure 10.- The effect of angle of attack upon the horizontal distance traveled along the flight path from the reentry point to the recovery point. $\gamma_o = -1^o$; W/S = 20 pounds per square foot.

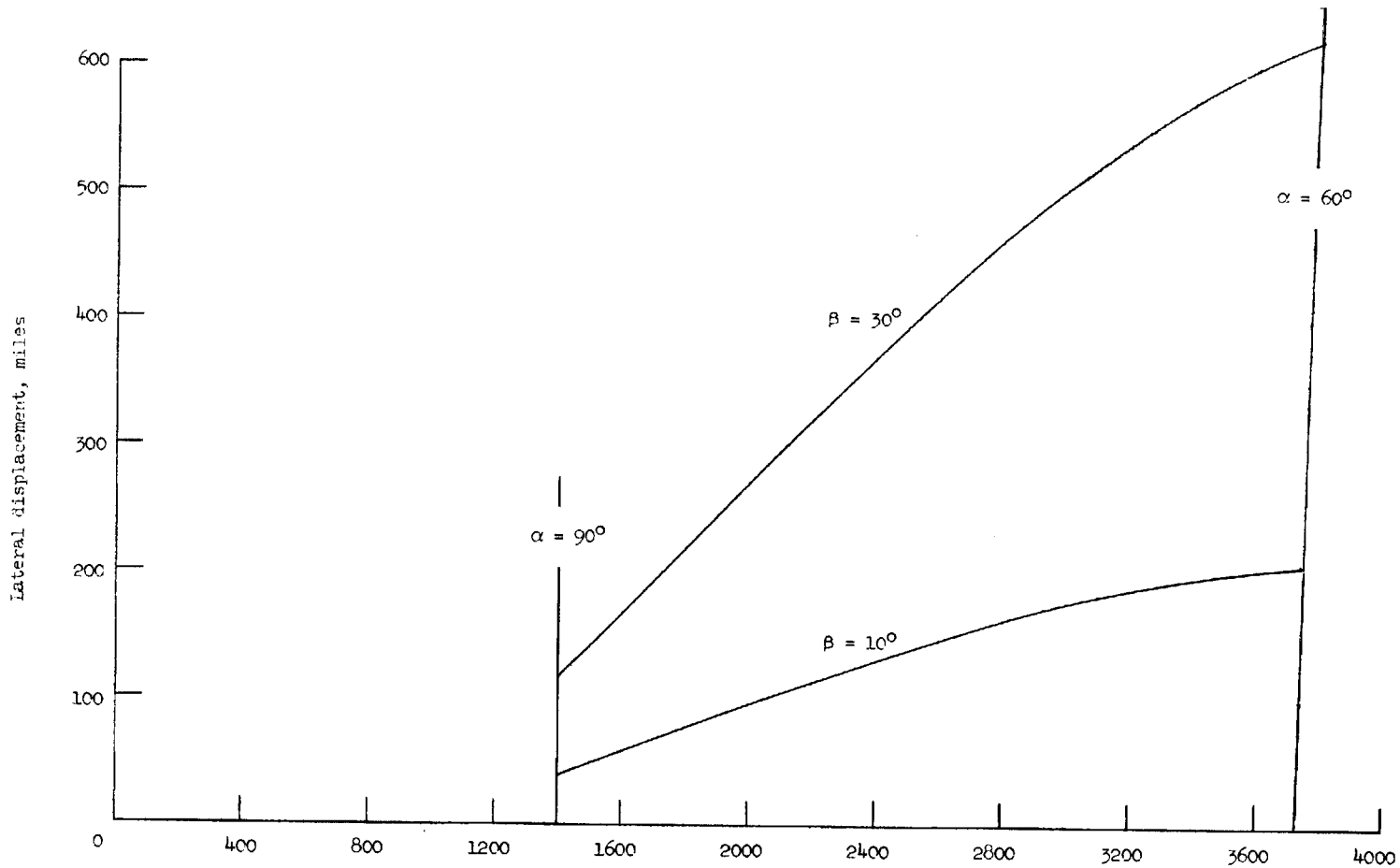


Figure 11.- The effect of angle of sideslip upon the lateral displacement of the flight path as a function of the distance traveled from the point of reentry to the point of recovery. $\gamma_o = -1^\circ$; W/S = 20 pounds per square foot.

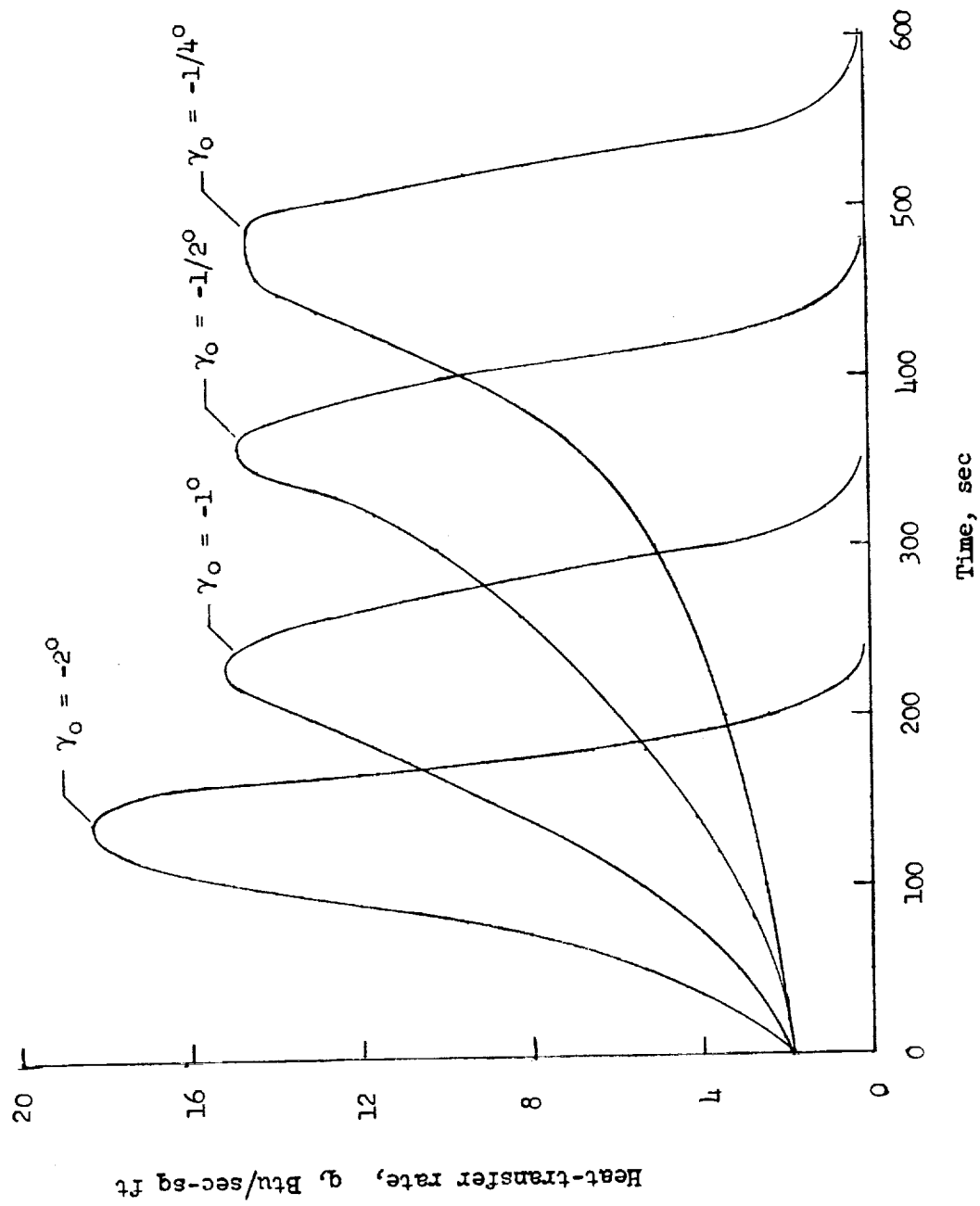


Figure 12.- Effect of the reentry angle $\gamma_o$ on the heat-transfer rates calculated for reentries at 90° angle of attack. W/S = 20 pounds per square foot; reentry altitude = 350,000 feet.

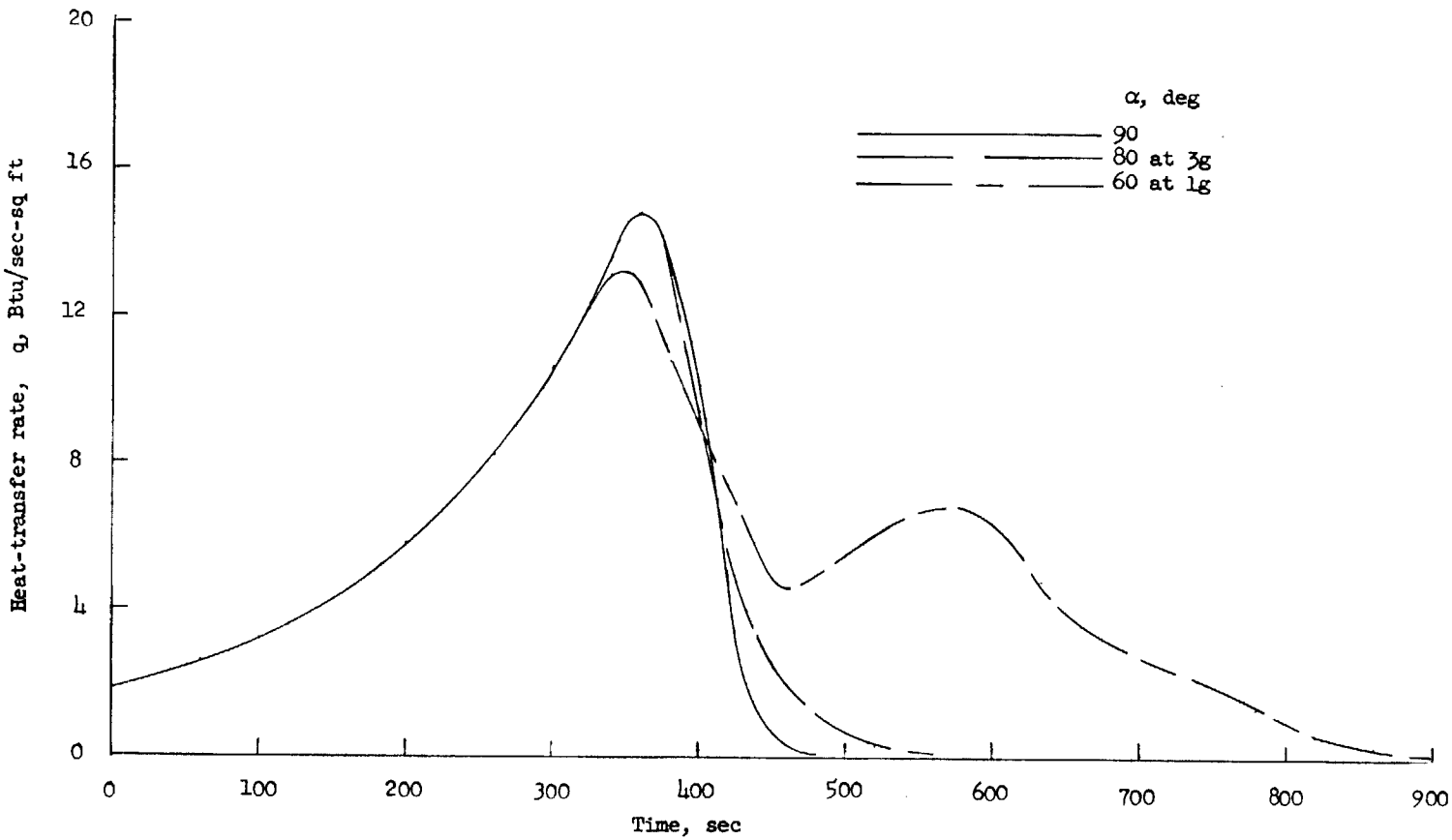


Figure 13.- Effect of different angle-of-attack programs on the heat-transfer rates calculated for trajectories having a reentry angle of -1/2°. W/S = 20 pounds per square foot; reentry altitude = 350,000 feet.

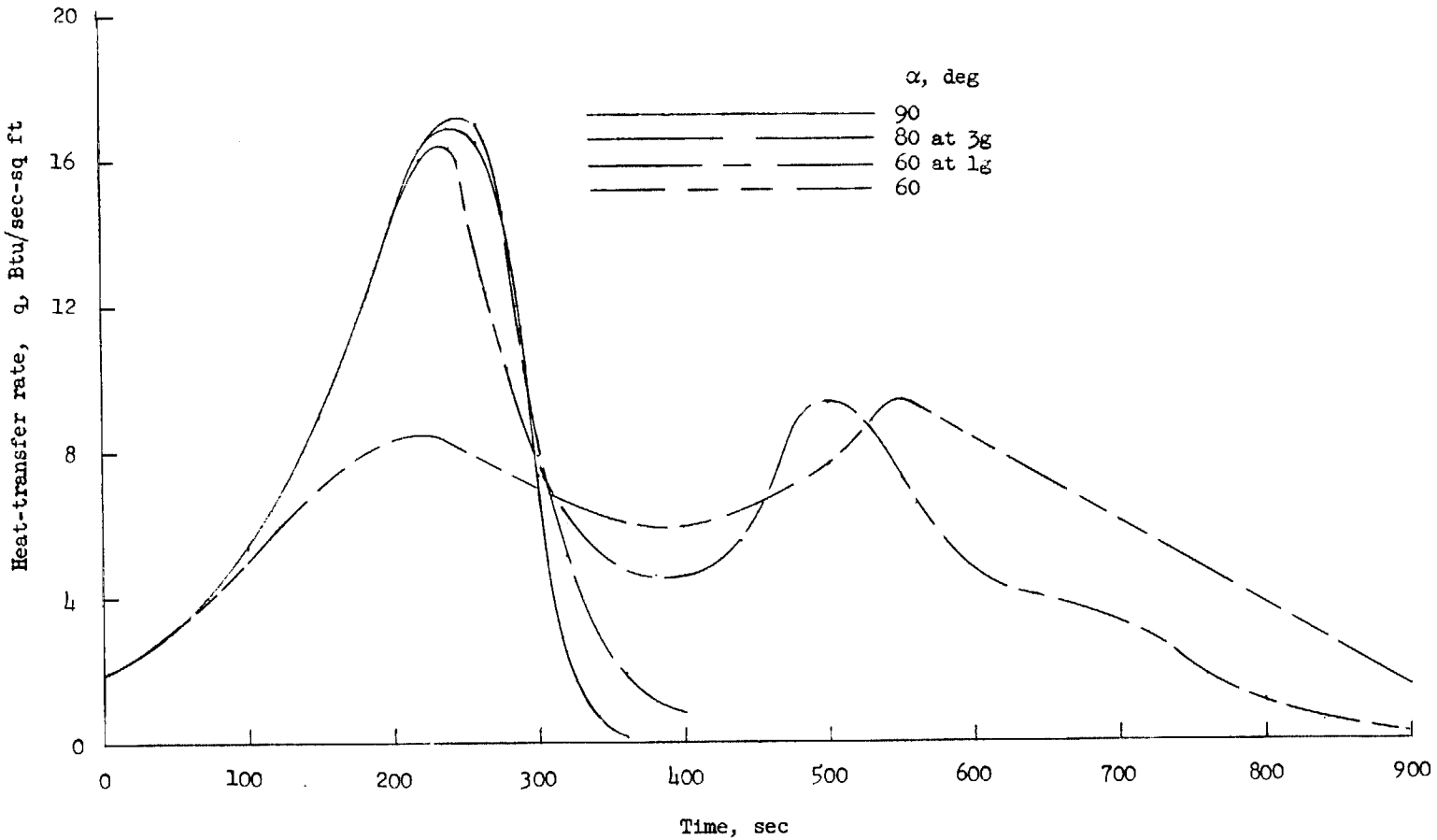


Figure 14.- Effect of different angle-of-attack programs on the heat-transfer rates calculated for trajectories having a reentry angle of $-1^{\circ}$. W/S = 25 pounds per square foot; reentry altitude = 350,000 feet.

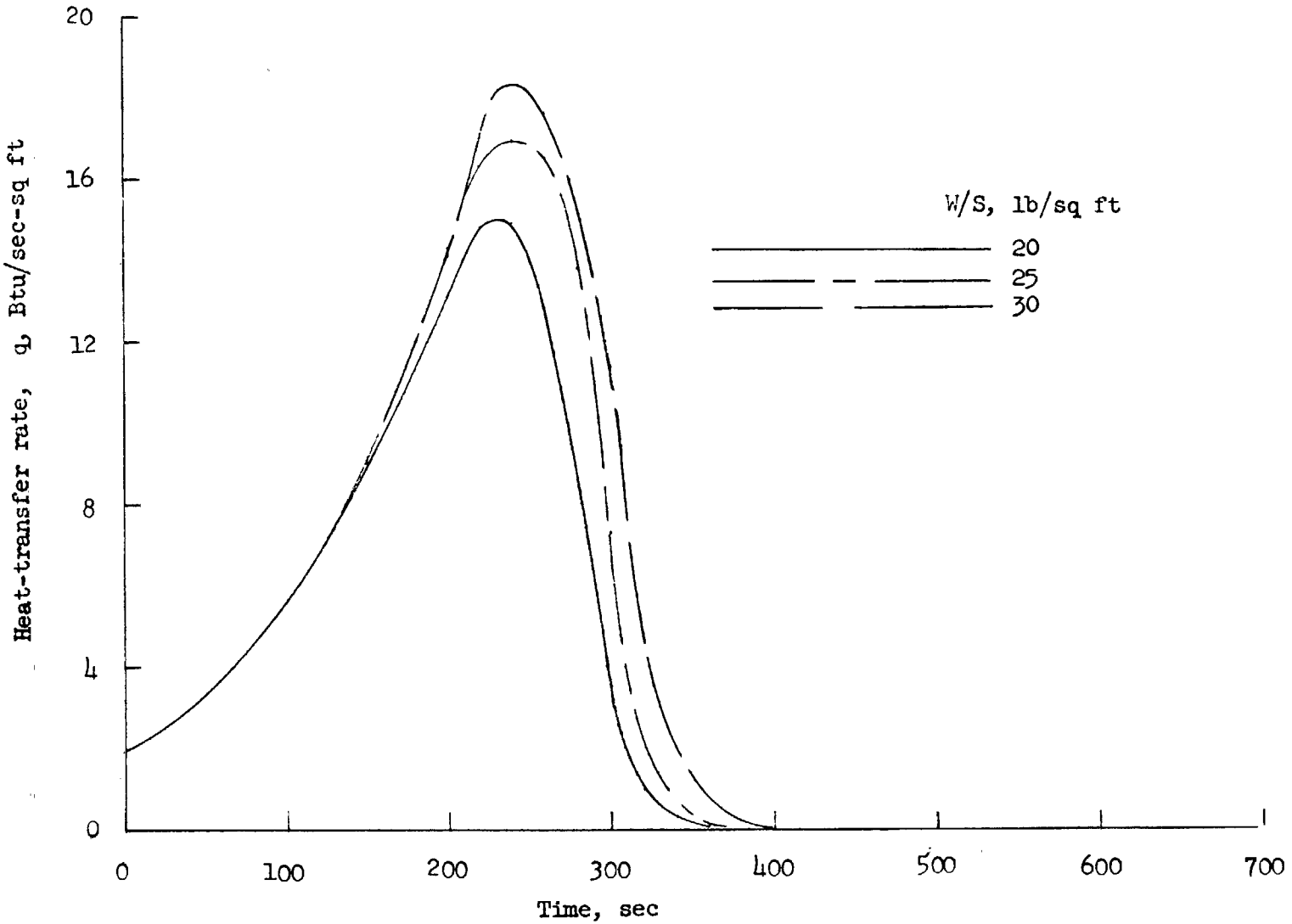


Figure 15.- Effect of wing loading W/S on the heat-transfer rates calculated for trajectories having a reentry angle of $-1^{\circ}$. $\alpha = 90^{\circ}$; reentry altitude = 350,000 feet.

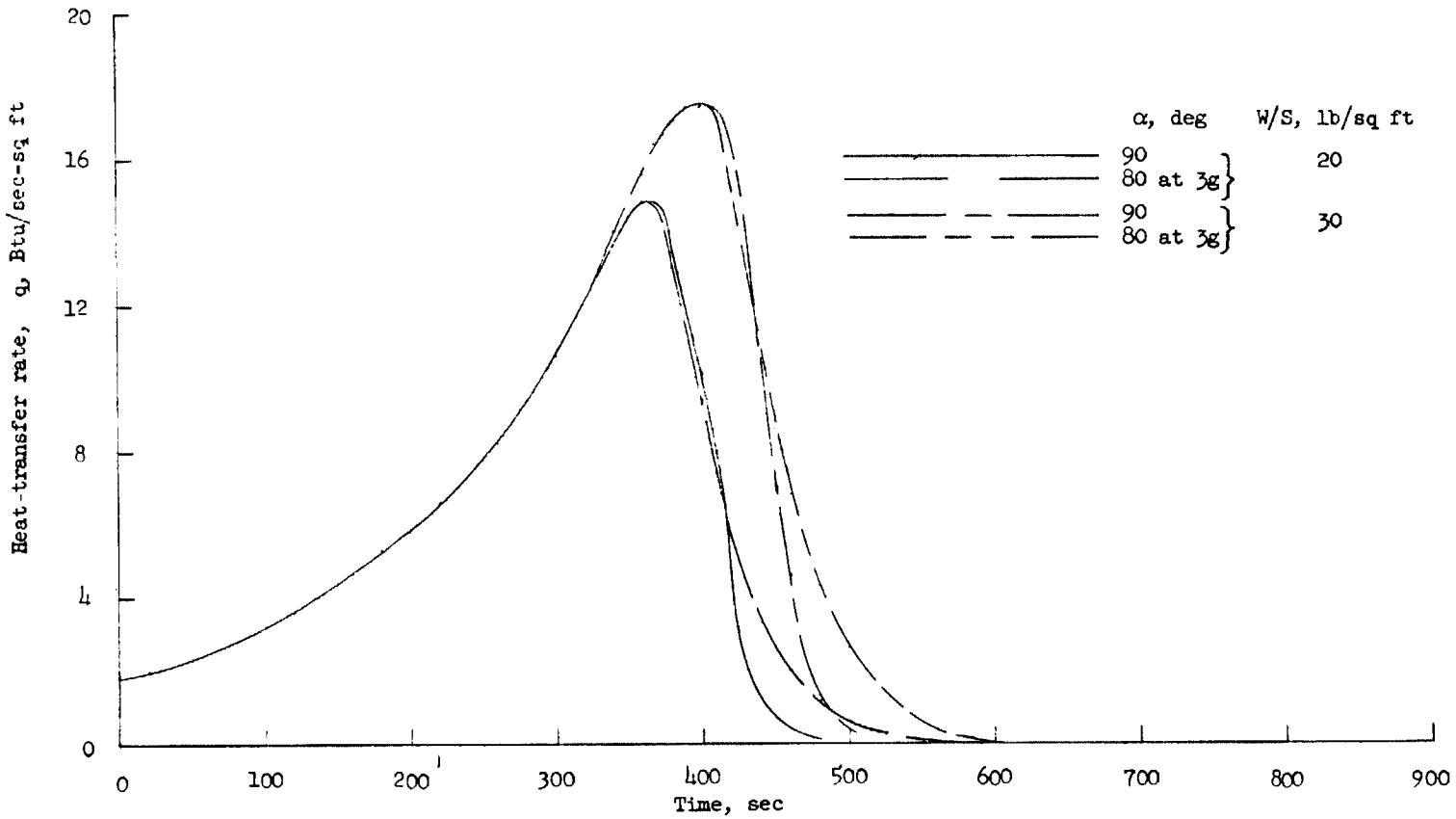


Figure 16.- Effect of wing loading W/S on the heat-transfer rates calculated for trajectories having a reentry angle of -1/2°. Reentry altitude = 350,000 feet.

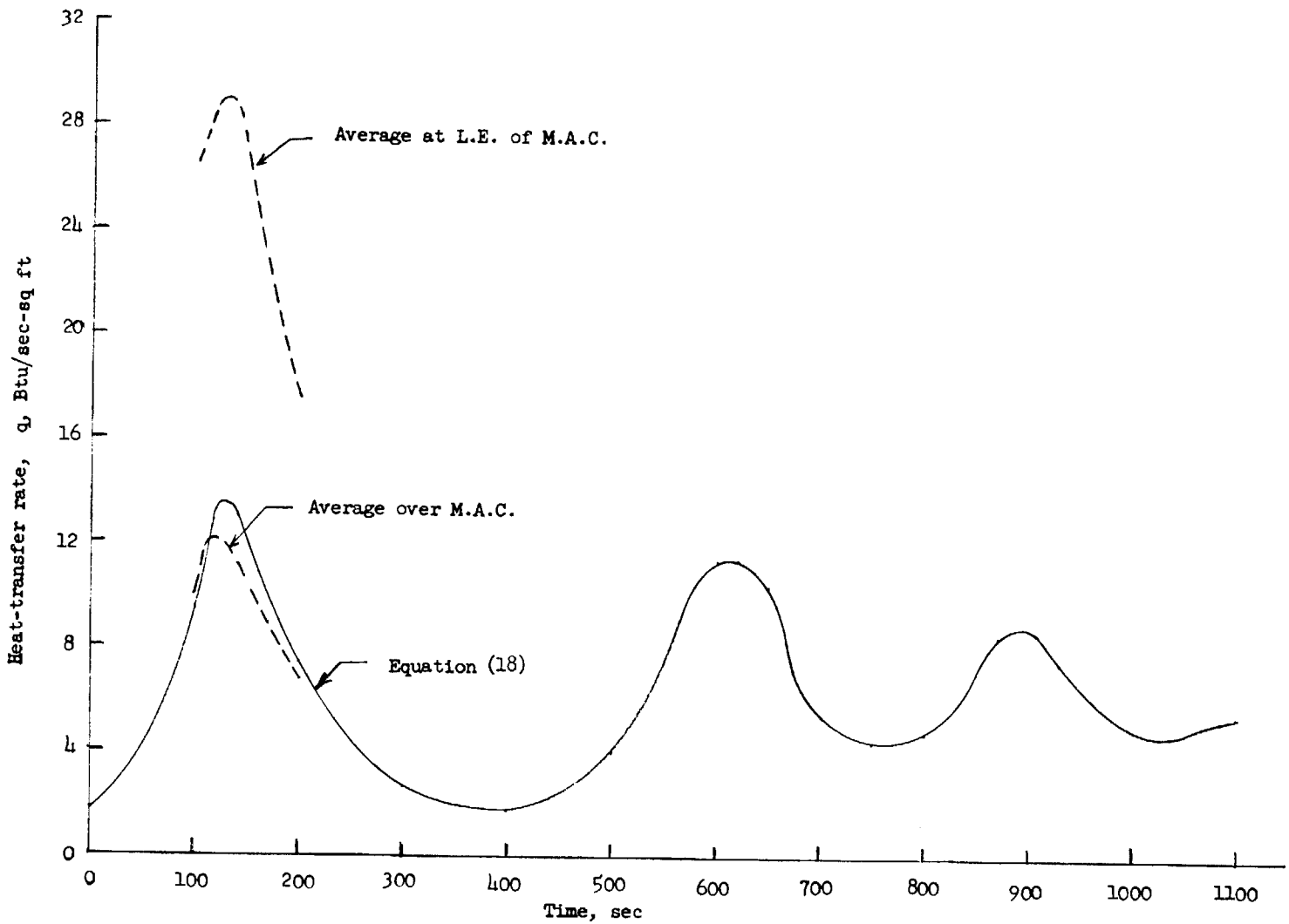


Figure 17.- Heat-transfer rates calculated for a trajectory having a reentry angle of $-2^{\circ}$. $\alpha = 43^{\circ}$; W/S = 20 pounds per square foot; reentry altitude = 350,000 feet.

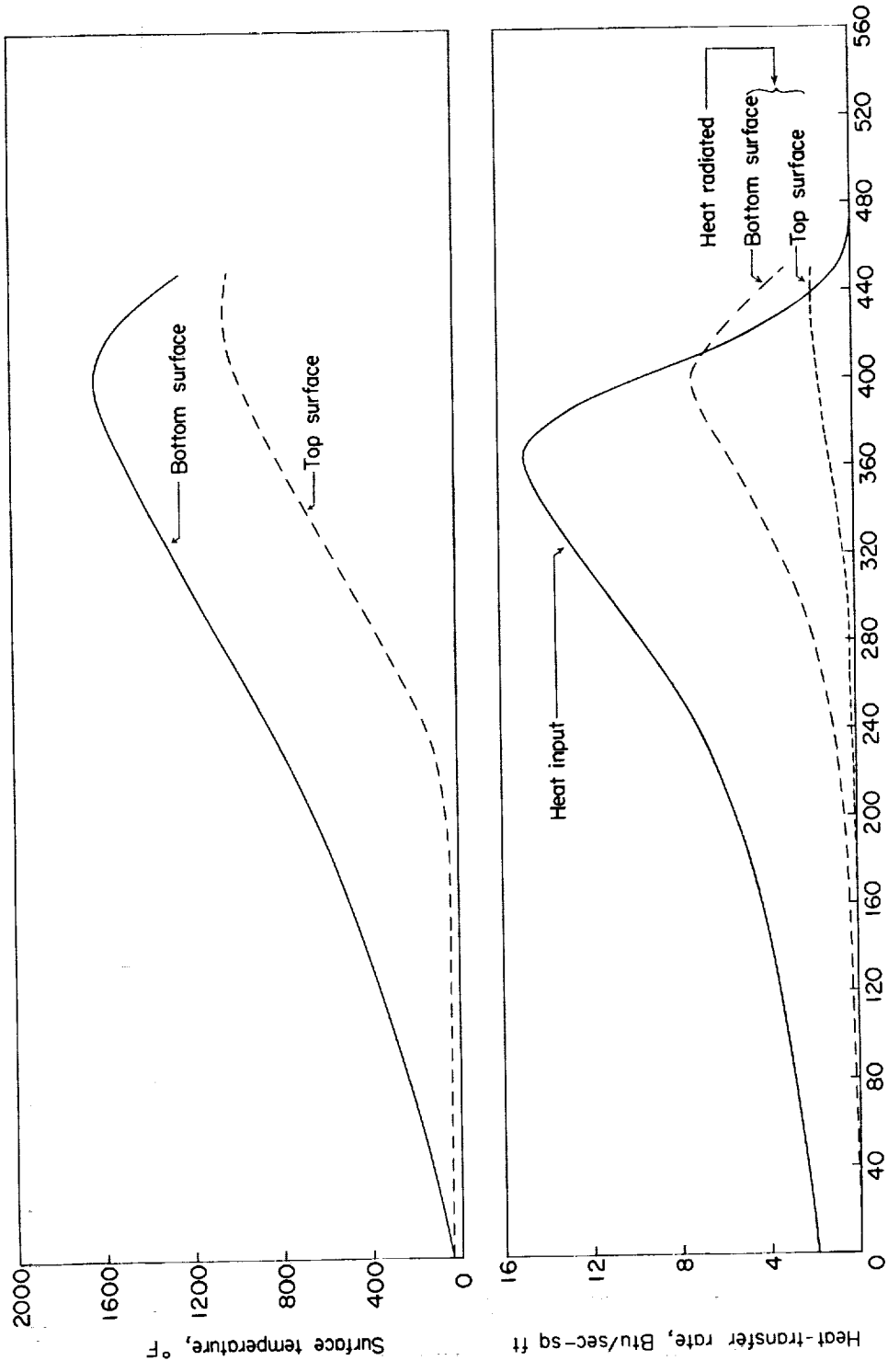


Figure 18.- Calculated time history of the temperatures of the top and bottom surfaces of the structure, the heat-transfer rate input, and the radiated heat-transfer rates of the top and bottom surface. $\gamma_o = -1/2^o$; $\alpha = 90^o$; W/S = 20 pounds per square foot.